

Elsevier Editorial System(tm) for Quaternary Science Reviews
Manuscript Draft

Manuscript Number:

Title: The 100-133 ka record of Italian explosive volcanism and revised tephrochronology of Lago Grande di Monticchio

Article Type: Research and Review Paper

Keywords: tephrochronology, Italian volcanism, Lago Grande di Monticchio, Eastern Mediterranean

Corresponding Author: Dr. Sabine Wulf,

Corresponding Author's Institution: Deutsches GeoForschungsZentrum

First Author: Sabine Wulf

Order of Authors: Sabine Wulf

Abstract: Laminated sediments of the maar lake Lago Grande di Monticchio in southern Italy exhibit a unique sequence of numerous primary tephra events that provide both insights into the Late Quaternary eruptive history of Italian volcanoes and an archive of essential marker horizons for dating and linking palaeoclimate records throughout the Eastern Mediterranean. The acquisition of new sediment cores from this lake now extends the existing 100 ka-tephra record back to 133 ka BP, the end of the penultimate Glacial. The additional ca. 30 m of sediments host a total number of 52 tephra fallout layers that have been identified on the basis of detailed geochemical and petrographical examinations. Tephras can be assigned to hitherto poorly known Plinian to sub-Plinian eruptions of the nearby Campanian (Ischia Island, Phlegrean Fields), Roman (Sabatini volcanic district) and Aeolian-Sicilian volcanoes (Etna, Stromboli, Salina) and are dated according to the varve and sedimentation rate chronology of Monticchio sediments. The most prominent tephra layers within the interval of investigation - TM-25 and TM-27 - can be firmly correlated with Ionian Sea tephras X-5 (ca. 105 ka BP) and X-6 (ca. 108-110 ka BP). Those in addition to 25 other tephra layers correlated with radiometrically and radioisotopically dated volcanic events provide the basis for a robust revised tephrochronology of the entire Monticchio sediment sequence for the last 133 kyrs.



Deutsches GeoForschungszentrum Potsdam -
Sektion 5.2 - Telegrafenberg D - 14473 Potsdam

Sektion 5.2
Klimadynamik und Landschaftsentwicklung

Dr. Sabine Wulf
Telegrafenberg
Haus C, Room 320
D-14473 Potsdam
Germany
Tel.: 49-(0)331-288 1381
Fax: 49-(0)331-288 1302
E-mail: swulf@gfz-potsdam.de

June, 14th, 2012

Dear editor,

please find enclosed the manuscript **The 100-133 ka record of Italian explosive volcanism and revised tephrochronology of Lago Grande di Monticchio** by Sabine Wulf, Jörg Keller, Martine Paterne, Jens Mingram, Stefan Lauterbach, Stephan Opitz, Gianluca Sottili, Biagio Giaccio, Paul Albert, Chris Satow, Marco Viccaro, Achim Brauer to be submitted to the Journal "Quaternary Science Reviews". This manuscript has not has not been previously published, wholly or in part in any other scientific journal and it has not been submitted to any other journal.

This paper is an important contribution to the late Pleistocene tephrostratigraphy in the Eastern Mediterranean as provided by the high-resolution sediment record of Lago Grande di Monticchio, southern Italy.

Please find below a list of suggested reviewers:

Dr. Christine Lane

Research Laboratory for Archaeology and the History of Art
Dyson Perrins Building, South Parks Rd, Oxford, OX1 3QY, U.K.

E-mail: christine.lane@rlaha.ox.ac.uk

Phone: +44-1865 285203

Fax: +44-1865 285220

Homepage: <http://www.arch.ox.ac.uk/CL1.html>

Dr. Roberto Sulpizio

Università degli Studi di Bari "ALDO MORO"
Dipartimento di Scienze della Terra e Geoambientali
Via Orabona, 4 - 70125 BARI, Italy
E-mail: r.sulpizio@geomin.uniba.it
Phone: +39-080 5442608
Fax: +39-080 5442625
Homepage: <http://www.geo.uniba.it/sulpizio.html>

Prof. Dr. John Lowe

Department of Geography
Royal Holloway, University of London
Egham Hill, EGHAM, Surrey TW20 0EX, U.K.
E-mail: J. Lowe@rhul.ac.uk
Phone: +44-1784 443565
Fax: +44-1784 472836
Homepage: http://pure.rhul.ac.uk/portal/en/persons/john-lowe_220fd6cc-d8c5-4016-bdf5-444bc9babdc1.html

Thank you for your consideration of this manuscript.

On behalf of the authors,
Sincerely

Dr. Sabine Wulf (corresponding author)

Highlights

Laminated sediments of the maar lake Lago Grande di Monticchio in southern Italy exhibit a unique sequence of numerous primary tephra events that provide both insights into the Late Quaternary eruptive history of Italian volcanoes and an archive of essential marker horizons for dating and linking palaeoclimate records throughout the Eastern Mediterranean. The acquisition of new sediment cores from this lake now extends the existing 100 ka-tephra record back to 133 ka BP, the end of the penultimate Glacial. The additional ca. 30 m of sediments host a total number of 52 tephra fallout layers that have been identified on the basis of detailed geochemical and petrographical examinations. Tephras can be assigned to hitherto poorly known Plinian to sub-Plinian eruptions of the nearby Campanian (Ischia Island, Phlegrean Fields), Roman (Sabatini volcanic district) and Aeolian-Sicilian volcanoes (Etna, Stromboli, Salina) and are dated according to the varve and sedimentation rate chronology of Monticchio sediments. The most prominent tephra layers within the interval of investigation - TM-25 and TM-27 - can be firmly correlated with Ionian Sea tephras X-5 (ca. 105 ka BP) and X-6 (ca. 108-110 ka BP). Those in addition to 25 other tephra layers correlated with radiometrically and radioisotopically dated volcanic events provide the basis for a robust revised tephrochronology of the entire Monticchio sediment sequence for the last 133 kyrs.

1
2
3
4
5
6
7
8
9
10
11
12
13
14
15
16
17
18
19
20
21
22
23
24
25
26
27
28
29
30

**The 100-133 ka record of Italian explosive volcanism and revised
tephrochronology of Lago Grande di Monticchio**

Sabine Wulf^{1*}, Jörg Keller², Martine Paterne³, Jens Mingram¹, Stefan Lauterbach¹, Stephan
Opitz⁴, Gianluca Sottili⁵, Biagio Giaccio⁵, Paul Albert⁶, Chris Satow⁶, Marco Viccaro⁷, Achim
Brauer¹

¹ GFZ German Research Centre for Geosciences, Section 5.2 – Climate Dynamics and
Landscape Evolution, Telegrafenberg, D-14473 Potsdam, Germany

² Institute of Geosciences, Mineralogy – Geochemistry, Albert-Ludwigs-University Freiburg,
Albertstrasse 23b, D-79104 Freiburg, Germany

³ Laboratoire des Sciences du Climat et de l'Environnement, CNRS-CEA, Gif-sur-Yvette,
France

⁴ Alfred Wegener Institute, Telegrafenberg A43, D-14478 Potsdam, Germany

⁵ Istituto di Geologia Ambientale e Geoingegneria IGAG-CNR, Rome Italy

⁶ Department of Earth Sciences, Royal Holloway, University of London, Egham, TW20 0EX,
United Kingdom

⁷ Dipartimento di Scienze Biologiche Geologiche e Ambientali, Università di Catania, Corso
Italia 57, I-95129, Catania, Italy

* Corresponding author: Tel.: +49-(0)331-2881381 Fax: 0049-(0)331-2881302.

E-Mail address: swulf@gfz-potsdam.de

31 **Abstract**

32 Laminated sediments of the maar lake Lago Grande di Monticchio in southern Italy exhibit a
33 unique sequence of numerous primary tephra events that provide both insights into the Late
34 Quaternary eruptive history of Italian volcanoes and an archive of essential marker horizons
35 for dating and linking palaeoclimate records throughout the Eastern Mediterranean. The
36 acquisition of new sediment cores from this lake now extends the existing 100 ka-tephra
37 record back to 133 ka BP, the end of the penultimate Glacial. The additional ca. 30 m of
38 sediments host a total number of 52 tephra fallout layers that have been identified on the basis
39 of detailed geochemical and petrographical examinations. Tephra layers can be assigned to hitherto
40 poorly known Plinian to sub-Plinian eruptions of the nearby Campanian (Ischia Island,
41 Phlegrean Fields), Roman (Sabatini volcanic district) and Aeolian-Sicilian volcanoes (Etna,
42 Stromboli, Salina) and are dated according to the varve and sedimentation rate chronology of
43 Monticchio sediments. The most prominent tephra layers within the interval of investigation -
44 TM-25 and TM-27 - can be firmly correlated with Ionian Sea tephra X-5 (ca. 105 ka BP) and
45 X-6 (ca. 108-110 ka BP). Those in addition to 25 other tephra layers correlated with
46 radiometrically and radioisotopically dated volcanic events provide the basis for a robust
47 revised tephrochronology of the entire Monticchio sediment sequence for the last 133 kyrs.

48

49 *Keywords:* tephrochronology, Italian volcanism, Lago Grande di Monticchio, Eastern
50 Mediterranean

51

52

53 **1. Introduction**

54 During the past decades, tephra studies in the Central Mediterranean facilitated the dating and
55 linking of several medial to distal terrestrial and marine palaeoenvironmental records leading
56 to a continuous development of detailed tephrostratigraphies of Italian explosive volcanism
57 for at least the last 100 kyrs (e.g., Keller et al., 1978; Paterne et al., 1986; Wulf et al., 2004;
58 Siani et al., 2004; Paterne et al., 2008; Lowe et al., 2007; Calanchi and Dinelli, 2008; Wulf et
59 al., 2008; Sulpizio et al., 2010).

60 Tephrostratigraphies, in general, require a completeness of major eruptive events, a
61 reliable dating, a clear stratigraphic order and an unambiguous identification of tephra layers, which
62 in combination are difficult to derive from a single archive. Proximal (near-vent) sites, for
63 instance, are ideal for dating tephra deposits, but may lack in complete stratigraphies due to
64 burial and erosion processes. Medial to distal environments may record only large-magnitude

65 eruptions and miss small-scale events, but have the potential to document the stratigraphic
66 interfingering and super-positioning of tephra from multiple volcanic sources. However, the
67 dating of tephra in distal sedimentary archives can be problematic due to the lack of datable
68 material. In this respect, annually laminated lake sediments are exceptionally valuable
69 archives since they provide both eruptive evidence from adjacent volcanic centres and robust
70 chronologies (e.g., Brauer et al., 1999; Wulf et al., 2004). In the central Mediterranean, such
71 an archive is given by the maar lake Lago Grande di Monticchio in southern Italy. A total of
72 293 visible tephra fallout layers from volcanic sources in central and southern Italy, which are
73 located in a distance from 100-540 km, were previously identified in the Monticchio
74 sediments providing a detailed tephrostratigraphy of the explosive volcanism in Italy for the
75 last 100 kyrs (Newton and Dugmore, 1993; Narcisi, 1996; Wulf et al., 2004; Wulf et al.,
76 2006; Wulf et al., 2008). Detailed studies created a large data set of chronostratigraphical and
77 geochemical information of individual tephra that are widely used as references for the
78 correlation and dating of other distal and proximal tephra deposits, so far (e.g., Lowe et al.,
79 2007; Bourne et al., 2010; Smith et al., 2011; Giaccio et al., submitted).

80 The extended sediment record from Lago Grande di Monticchio (Brauer et al., 2007) exhibits
81 another 52 tephra layers providing a previously undocumented record of Italian volcanism for
82 the period 100-133 ka BP. Petrographies and geochemistries of the tephra are described and
83 interpreted in this paper. The ages of tephra deposition are provided by a combination of new
84 varve counting for the extended 30 m section and a partial revision of the varve and
85 sedimentation chronology of the <100 ka profile (Brauer et al., 2007). These data contribute
86 to the establishment of a reliable tephrostratigraphical record in the Central Mediterranean.

87

88 *Please place here Figure 1.*

89

90 **2. The study site**

91 Lago Grande di Monticchio (40°56'N, 15°35'E, 656 m a.s.l.) is located about 120 km east of
92 Naples in the Monte Vulture volcanic complex in the region of Basilicata, southern Italy (Fig.
93 1a). It is the larger of two adjacent maar lakes that were formed during the final
94 phreatomagmatic eruptions of Monte Vulture at 132 ± 12 ka BP (Lago Grande di Monticchio;
95 Brocchini et al., 1994; Stoppa and Principe, 1998) and 141 ± 11 ka BP (Lago Piccolo di
96 Monticchio; Villa and Buettner, 2009), respectively. Lago Grande di Monticchio has a total
97 surface area of 0.4 km², a maximum water depth of 36 m, and has no major in-or outflows
98 (Fig. 1b).

99 With a distance of 100-350 km, the site is close and in a favourable downwind position to the
100 active volcanoes of the alkaline Roman Co-magmatic Province (RCP). The RCP is subdivided
101 into the Campanian and Roman volcanic area. The Campanian Province includes the
102 stratovolcanoes of Monte Vulture, Roccamonfina, Somma-Vesuvius, the Phlegrean Fields and
103 the Islands of Ischia, Procida-Vivara and Ponza. Some of those centres were active until the
104 recent past, for instance Vesuvius (<39 ka BP; De Vivo et al., 2001), the Phlegrean Fields
105 (≤ 60 ka BP; Pappalardo et al., 1999) and Ischia (<150 ka BP; Poli et al., 1989). Activities of
106 Procida-Vivara and Roccamonfina ceased at ca 14 ka BP (Scandone et al., 1991) and 130 ka
107 BP (Radicati di Brozolo et al., 1988), respectively. Volcanism in the Roman Province is older
108 than in the Campanian area. The youngest tephra producing eruptions are known from the
109 Alban Hills (560 to 33 ka BP; Giaccio et al., 2009; Marra et al., 2011), the Sabatini Volcanic
110 District (800 to 86 ka BP; Sottili et al., 2010) and the Vico volcanic centre (≥ 420 to 95 ka BP;
111 Laurenzi and Villa, 1987; Sollevanti, 1983). Activity of both the Campanian and Roman
112 volcanic provinces produced huge amounts of tephra fallout, mainly K-alkaline trachytic-
113 phonolitic in composition. Lago Grande di Monticchio is furthermore located 280 to 540 km
114 northeast of the active volcanic centres of the Aeolian Islands (280 km), Mount Etna (360 km)
115 and the Island of Pantelleria in the Strait of Sicily (550 km). Erupted material of these
116 volcanoes ranges in composition from calcalkaline (Aeolian Islands) to Na-pronounced
117 alkaline to mugearitic and pantelleritic (Etna, Pantelleria). Some of these eruptions were high-
118 explosive, and the erupted tephra material was widely dispersed in the Central Mediterranean
119 (e.g., Keller et al., 1978; Paterne et al., 1986; Vezzoli, 1991; Paterne et al., 2008).

120

121 *Please place here Figure 2.*

122

123 **3. Material and Chronology**

124 Lago Grande di Monticchio is a site of intense studies for palaeoclimate reconstruction since
125 the early 1980's. A first sediment core of 25.5 m was taken in a fen at the western margin of
126 the lake (Watts, 1985). Three further coring campaigns were carried out within the lake basin
127 of Lago Grande di Monticchio in the years 1990, 1994 and 2000 recovering eight overlapping
128 sediment cores. The first sediment recovery in 1990 exhibited a sediment record of ca. 52 m
129 total length using three parallel cores from shallow water depths of 5-6 m (cores LGM-B,
130 LGM-D, LGM-E; Fig.1b). Counting of varved sections and calculating sedimentation rates in
131 sections of poor varve preservation dated the base of this composite sequence at 76,344
132 calendar years BP (1950) (Zolitschka and Negendank, 1996). Initial tephrochronological

133 results and ¹⁴C dates of terrestrial plant material in the sediments corroborated the upper part
134 of the varve and sedimentation rate chronology (Newton and Dugmore, 1993; Narcisi, 1996;
135 Zolitschka and Negendank, 1996). Two new cores, LGM-L and LGM-J, from a slope at 2.3 m
136 water depth and the deeper central part at 13.5 m water depth, respectively, were recovered
137 during a coring campaign in 1994 (Fig. 1b). The longer core LGM-J was used to extend the
138 existing LGM-B/D/E profile to a total length of 72.5 m. The base of the composite profile
139 LGM-B/D/E/J has been varve dated at 101,670 calendar years BP (Brandt et al., 1999). An
140 independently dated tephrochronology of this profile confirmed the varve and sedimentation
141 rate chronology in overall with a mean deviation of 5%, though there were some larger
142 deviations at the extended lower part of the profile indicating missing sediments (Wulf et al.,
143 2004). A third field campaign was initiated in August/September 2000 providing three longer
144 and overlapping cores, LGM-M, LGM-N and LGM-O, from sites close to core LGM-J (Fig.
145 1b). Core LGM-O most likely reached the base of lacustrine deposits, which is characterized
146 by pyroclastic gravel of the final Monte Vulture volcanic activities (maar lake formation). A
147 new composite profile, LGM-B/D/E/J/M/O, was established providing a total length of 103.1
148 m of sediments (Brauer et al., 2007). Varve counting of the extended >101,670 years section
149 (core LGM-M and LGM-O) as well as a re-evaluation of varve counts in two short sections
150 overlapping the lower part of the LGM-J core and in the upper LGM-B/D section between
151 11.17 m (19,280 calendar years BP) and 26.48 m composite depth yield a basal age of lake
152 deposits of 132,900 calendar years BP (Brauer et al., 2007). As a result, time constraints of
153 tephra deposits older than 19,280 calendar years BP published in Wulf et al. (2004) and Wulf
154 et al. (2006) have to be revised (see Table 4).

155 The extended sediment section between 72.5 m (re-dated at 105,280 calendar years BP) and
156 103.1 m (132,900 calendar years BP; Brauer et al., 2007) contains a total of 52 visible, distal
157 tephra layers that range in thickness between 0.2 mm and >2 m (Fig. 2). Host sediments of
158 these ash layers are organo-clastic muds that are annually laminated for the entire section
159 except for the lowermost part (>131 ka BP), which is characterized by the intercalation of
160 thick turbidites (Brauer et al., 2007). Detailed studies of tephtras were performed including
161 petrographical, geochemical and grain size analyses.

162

163 *Please place here Table 1.*

164

165 **4. Tephrochronological Methods**

166 Tephra layers are labelled in accordance to Wulf et al. (2004) and Wulf et al. (2006) as tephra
167 marker “TM” with the respective ascendant numbers starting from the youngest of the >100
168 ka tephtras (TM-25) to the oldest deposit (TM-42). Tephra layers were described in respect to
169 their mineral/lithic assemblage, maximum grain sizes and thicknesses using large-scale thin
170 sections of in-situ sediment blocks (Brauer et al., 2000). The major-element composition of
171 volcanic glass was analysed on polished thin sections of loose tephra material that was
172 extracted and cleaned with a 10% hydrogen peroxide solution. Electron probe microanalyses
173 (EPMA) were carried out at the GFZ German Research Centre of Geosciences in Potsdam
174 using a Cameca SX-100 electron microprobe (WDS). Measurements were obtained at 15 kV
175 (accelerating voltage) and 20 nA (beam current) with beam sizes of 15 µm or 20 µm. Peak
176 counting times were 20 s for each element, except for Na (10 s). Between 5 and 22 glass
177 shards were analysed per tephra layer. Instrumental calibration used interlaboratory natural
178 mineral and glass reference materials such as the Lipari obsidian (Hunt and Hill, 1996)
179 (supplementary table A). Tephtras TM-24a, TM-24b (Wulf et al., 2004) and TM-27 were
180 additionally analysed using a JEOL 8600 wavelength-dispersive electron microprobe in the
181 Research Laboratory for Archaeology and the History of Art, University of Oxford, U.K. An
182 analytical setup was chosen at 15 kV acceleration voltage, 6 nA current and 10 µm beam
183 diameter. Element analysis times were 30 s for each element, except for P and Cl (60 s), and
184 Na (10 s). Glass reference materials used Atho-G and StHs6/80-G (Supplementary Table B).
185 EPMA analyses showing totals lower than 95 wt% were excluded from either data set.
186 Petrological classification of tephtras was based on normalized data of the glass major-element
187 composition using the Total-Alkali-Silica diagram after Le Bas et al. (1986). Tephra
188 compositional data are summarized in Tables 1 and 2 and provided in full in the
189 Supplementary Table A and B.

190 EPMA glass data of Monticchio tephtras were compared with SEM-EDS glass data of marine
191 tephtras from Tyrrhenian and Ionian Sea sediment cores (Paterne, 1985; Paterne et al., 2008;
192 this study). Here, major elements of individual glass shards of tephtras were measured on a
193 JEOL/EDS instrument (core DED 87-08; see details Paterne et al., 2008) and on a
194 CAMEBAX/SEM equipment (cores KET 80-04 and KET 82-22; see details Paterne, 1985;
195 Paterne et al., 1986; Paterne et al., 1988; Paterne et al., 2008) at CNRS-CEA, Gif-sur-Yvette,
196 France.

197

198 *Please place here Figure 3.*

199

200 **5. Results**

201 In the following, detailed compositional and chronostratigraphical descriptions of each tephra
202 occurring in the 100-133 ka BP section are given, starting from the youngest to the oldest
203 deposit, and potential eruptive sources are discussed (see also Table 1). Calendar ages for
204 tephtras are provided according to the Monticchio varve and sedimentation rate chronology
205 after Brauer et al. (2007).

206

207 **TM-25** is an 11.3 cm thick and coarse-grained (max. 1.5 mm) white pumice fallout in 74.11
208 m composite depth. It is dated by the Monticchio varve and sedimentation rate chronology at
209 105,480 calendar years BP. Large phenocrysts of sanidine, zoned plagioclase, biotite,
210 amphibole, green clinopyroxene, and olivine xenocrystals are common in this tephra (Fig. 3a).
211 Apatite often occurs as micro-crystal inclusion in juvenile clasts. Minor amounts of volcanic
212 lithics and altered tuffs are also visible. Pumice fragments are highly vesicular (Fig. 3a) and
213 show a K-trachytic composition with alkali ratios of 2. The tephra layer is mixed with fine
214 organic sedimentary material towards the top of the deposit. Based on the relatively
215 homogenous chemical composition (Fig. 4a), the large grain sizes and the matching time
216 constraint, we propose a correlation of TM-25 with the marine X-5 tephra. The widely
217 distributed tephra layer X-5 (and the associated X-6) have been defined as first-order marker
218 beds in the marine record of the Ionian Sea by Keller et al. (1978), and later confirmed by
219 new sediment cores of the Meteor-cruise M25-4 (Keller et al., 1996; Kraml, 1997; Keller and
220 Kraml 2004; Scheld, 1995). For X-5, a $^{40}\text{Ar}/^{39}\text{Ar}$ date of 105 ± 2 ka has been obtained by
221 Kraml (1997) in accordance with its position directly below sapropel S-4 and with the marine
222 oxygen isotope curve (e.g., Allen et al., 1999). The composition of X-5 points to a
223 Campanian origin (Keller et al., 1978; Morche, 1988; Scheld, 1995, Keller and Kraml, 2004;
224 Di Vito et al., 2008; Giaccio et al., submitted), but the proximal source of X-5 has not been
225 defined yet. In the Tyrrhenian Sea an equivalent tephra marker, C-27, of Paterne (1985) and
226 Paterne et al. (2008) is correlated with the X-5 tephra. The prominent layer X-5 (and the
227 closely related X-6) have also been identified in terrestrial archives of Central and Southern
228 Italy (Morche 1988; Lucchi et al. 2008; Marciano et al., 2008; Giaccio et al., submitted).

229

230 **TM-26** is a 1 mm thick, fine-grained, grey-brownish ash layer in 74.47 m composite depth
231 that is dated at 106,300 calendar years BP. It is dominated by loose crystals of plagioclase,
232 orthopyroxene, greenish clinopyroxene, rare sanidine, olivine, amphibole, Fe-Ti-oxides, and

233 abundant tachylites. Glass shards are light and brown in colour, low to moderate vesicular and
234 often rich in apatite microcrysts. The glass chemical data reflect a heterogeneous Na-
235 pronounced trachydacitic composition showing high SiO₂ concentrations of ca. 65 wt%
236 (normalized data). Such a glass composition is known from younger pyroclastics of Mount
237 Etna, i.e. from the Biancavilla/Y-1 tephra (17.3 ka BP) (Fig. 4b), and therefore we propose a
238 correlation of TM-26 with an older Plinian eruption of this volcano. Explosive behaviour of
239 Mount Etna during the considered time period of >100 ka BP developed during activities of
240 the Valle del Bove centres and the Timpe Phase (Coltelli et al., 2000; Branca et al., 2008;
241 Nicotra et al., 2011), and include the units of the Ancient Alkaline Centres (220 to 100 ka BP)
242 and Trifoglietto (100 to 60 ka BP) previously defined by Romano (1982). Based on the
243 comparison with bulk rock geochemical data we assume a correlation of TM-26 with the
244 proximal pyroclastics of the “Salto della Giumenta Unit” that has been assigned to activities
245 of the “Tardereria” volcano (Nicotra et al., 2011). This correlation is further supported by a
246 ⁴⁰Ar/³⁹Ar age of 105.8 ± 4.5 ka BP obtained from the groundmass of related lava flows of the
247 Tardereria activities (Branca et al., 2008), which is in good agreement with the varve age of
248 TM-26.

249

250 *Please place here Figure 4a and 4b.*

251

252 **TM-27** positioned in 78.85 m composite depth and dated at 108,330 calendar years BP is one
253 of the most prominent tephra deposits in the Monticchio sequence. Its base encompasses a 1.6
254 cm thick coarse-grained (max. 1.3 mm) pumice fallout that is overlain by ca. 2 m of finer
255 grained, vitric ash. Due to its small grain sizes the vitric ash is interpreted as a co-ignimbrite
256 that is mixed with lacustrine sedimentary material towards the top of the deposit. The basal
257 fallout is composed of highly vesicular, colourless to light brownish pumice fragments,
258 abundant phenocrysts of sanidine, biotite, plagioclase, clinopyroxene and amphibole as well
259 as fragments of older volcanic rocks and limestones (Fig. 3c). Juvenile clasts are phonolitic to
260 trachytic in composition and show a heterogeneous character in respect to CaO concentrations
261 (1.6 to 2.1 wt%) and K₂O/Na₂O ratios (0.9 to 1.4). The glass composition of TM-27 matches
262 that of the marine X-6 tephra (Fig. 4a), which forms a prominent marker horizon in the deep-
263 sea sediments of the Ionian Sea (Keller et al., 1978; Morche, 1988). The age of X-6 is
264 constrained by interpolation of the sapropel chronology of the Ionian Sea between sapropels
265 S4 and S5 at ca. 108-110 ka BP (Keller et al., 1978; Kraml, 1997; Keller and Kraml, 2004)
266 and is in good agreement with the varve age of tephra TM-27. The origin of X-6 is still under

267 discussion. Composition, thickness and maximum grain sizes in the Monticchio record,
268 however, strongly support the assumption of an origin of the X-6 tephra from nearby
269 Campanian volcanoes (Keller et al., 1978; Keller and Kraml, 2004; Marciano et al., 2008;
270 Giaccio et al., submitted). However, the exact Campanian source volcano of X-6 remains still
271 open.

272

273 **TM-28** consists of two distinct vitric ash layers of similar composition in 81.44 m (110,410
274 calendar years BP) and 81.53 m composite depth (110,830 calendar years BP). The upper
275 tephra TM-28a is a 2.1 cm thick and relatively fine-grained layer. Its phenocryst content
276 comprises sanidine, anorthoclase, biotite and orange-brown amphibole. Juvenile clasts of
277 quenched crystals dominate the top part of this deposit. The lower tephra TM-28b is only 2
278 mm thick and reveals coarser grain sizes (max. 400 μm). The mineral assemblage is made up
279 of sanidine, plagioclase, biotite, green Ti-augite and brown amphibole phenocrystals. Clasts
280 of quenched crystals and intermediate lava rock fragments are common as well. Highly
281 vesicular, brownish juvenile clasts characterize both tephra layers. Their trachytic to
282 phonolitic composition resembles that of tephra TM-27/X-6 (Fig. 4a). We therefore assume a
283 correlation of tephra layers TM-28 with a preceding undefined eruption from the same
284 Campanian source.

285

286 *Please place here Table 2.*

287

288 **TM-29 and TM-30** comprise a total of four eruptive sequences (TM-29-1, TM-29-2, TM-30-
289 1 and TM-30-2) of similar composition, each made up of multiple distinct tephra fallout
290 layers. Each sequence reflects a magma fractionation from more silicic to mafic rock
291 composition (Fig. 4c).

292 The uppermost tephra succession **TM-29-1** in 81.69 m to 81.91 m composite depth is
293 dated between 111,480 and 112,460 calendar years BP. It is made up of nine 0.2-5 mm thin,
294 grey-brownish ash layers labelled as TM-29-1a to TM-29-1i. All tephra layers contain light-
295 brownish, non- to low-vesicular, blocky glass shards. The glass composition is heterogeneous
296 latitic, basaltic-andesitic, tephriphonolitic to phonotephritic for the five basal layers (TM-29-
297 1e to TM-29-1i) and homogenous phonotephritic for the four top layers (TM-29-1a to TM-29-
298 1d). SiO_2 values decrease from the basal to the top layer from 54.6 to 49.7 wt%. Alkali totals
299 are low (7.9–10.8 wt%), while the $\text{K}_2\text{O}/\text{Na}_2\text{O}$ ratios show high values of 1.7–2.7. Abundant
300 phenocrysts of anorthoclase, pale greenish clinopyroxene, biotite as well as leucite and apatite

301 microcrystals are present in all layers. Lithic fragments comprise lavic rocks, greenish tuffs,
302 tachylites and clasts of quenched crystals. A remarkable decrease of lithic and phenocryst
303 concentration is visible from the basal (TM-29-1i) to the top deposits (TM-29-1a).

304 The underlying tephra succession **TM-29-2** is made up of eight distinct grey-brownish
305 tephra layers occurring between 82.06 m and 82.20 m composite depth and dated between
306 112,520 and 113,020 calendar years BP. The mineral and lithic assemblage is equivalent to
307 that of tephra succession TM-29-1. Glasses are also brownish in colour, blocky and low-
308 vesicular, but show a slightly more differentiated trachytic to basaltic trachyandesitic
309 composition (Fig. 4c). SiO₂ values range from 60.4 to 51.6 wt% from the basal to the top
310 layer. Within all layers, tephra components are set in a grey-brownish fine ashy matrix.

311 The next underlying tephra succession **TM-30-1** contains six grey to black-brownish
312 tephra layers (TM-30-1a to TM-30-1f) between 82.26 m and 82.67 m composite depth that
313 are dated between 113,370 and 114,000 calendar years BP. The basal layer of 12 mm
314 thickness is the lightest and most coarse-grained (<700 µm) tephra deposit within TM-30-1. It
315 comprises both high-vesicular, light pumice fragments and green-brownish, non- to low-
316 vesicular, blocky glass shards with abundant apatite microcrystals (Fig. 3b). The two types of
317 juvenile clasts reflect a bimodal chemical composition. Brown glass shards are concentrated
318 in the younger five tephra layers TM-30-1a to TM-30-1e and expose a latitic composition.
319 Mean SiO₂ concentrations are between 56.4 and 57.9 wt% (Fig. 4c). Light pumices, in turn,
320 are abundant in the basal layer TM-30-1f, and are homogenous trachytic in composition with
321 SiO₂ values of about 60 wt%. In addition, tephra particles of the uppermost tephras TM-30-1a
322 and TM-30-1b are embedded in a dark-brownish, ashy matrix. The mineral assemblage of all
323 layers of the succession TM-30-1 consists of large crystals of zoned plagioclase, sanidine,
324 biotite, greenish clinopyroxene and rare olivine xenocrysts; leucite and apatite microcrystals
325 in the juvenile phase occur as well. Lithics are abundant and encompass lavic rock fragments,
326 tachylites, altered greenish tuffs, clasts of quenched crystals and feldspar cumulates.

327 Tephra succession **TM-30-2** is deposited between 82.74 and 82.78 m composite depth
328 and date between 114,440 and 114,720 calendar years BP. TM-30-2 comprises four distinct
329 tephra layers of which the basal tephra TM-30-2d is the most prominent and coarse-grained
330 layer. It consists of two types of juvenile clasts characterized by a distinct chemical
331 composition: a) light, high-vesicular pumice fragments - rich in Fe-Ti-Oxide microcrysts -
332 showing a trachytic composition and b) rare brownish, low to moderate-vesicular glass shards
333 of trachyandesitic composition that are more dominant in the overlying tephras TM-30-2a to
334 TM-30-2c (Fig. 4c). Phenocrysts of all tephras of succession TM-30-2 encompass zoned

335 plagioclase, sanidine, light-greenish clinopyroxene, biotite and apatite. Lithics are abundant
336 and comprise older tuffs (altered pumices and tachylites with leucite inclusions), mafic to
337 intermediate volcanic rocks and clasts of quenched crystals.

338 According to their chemical composition, lithology and time of deposition between ca.
339 111 – 115 ka BP, successions TM-29 and TM-30 can be correlated with the TAU1-b pumice
340 fallout deposit occurring in medial-distal outcrops in the Campanian Plain and tentatively
341 attributed to an unknown Phlegrean Field eruption (Di Vito et al., 2008). This pyroclastic unit
342 consists of a well-sorted lapilli deposit made up of both light- and dark-coloured pumices that
343 show a widely variable composition from latitic to trachytic, similar to those of TM-29 and
344 TM-30 (Fig. 4c). The TAU1-b deposit is indirectly dated between the Tyrrhenian Sea high
345 stand (125 ka BP) and the Campanian Ignimbrite (ca. 39 ka BP) (Di Vito et al., 2008).

346

347

348 **TM-31** is a 0.5 mm thin fine-grained, white vitric ash layer in 82.79 m composite depth,
349 which is directly underlying the basal tephra of TM-31-2. It is dated by varve counting at
350 114,770 calendar years BP. TM-31 comprises both colourless, high-vesicular pumice
351 fragments of heterogeneous dacitic–trachydacitic composition (63 - 68 wt% SiO₂; K₂O/Na₂O
352 ratios of 2.3 to 3.6; alkali totals 6.0 - 8.7 wt%) and moderate-vesicular glasses of
353 phonotephritic to basaltic trachyandesitic composition (ca. 52 wt% SiO₂) (Fig. 4c). Only a
354 few loose crystals of plagioclase, sanidine, biotite and clinopyroxene as well as clasts of
355 quenched crystals occur. The mafic glass composition of TM-31 resembles that of tephra
356 successions TM-29 and TM-30, and therefore we suggest a correlation with both the same
357 Campanian source and the TAU1-b eruptive event.

358

359 **TM-32** is a 1 mm thin, fine-grained and light-brownish ash layer in 82.85 m composite depth.
360 It is dated at 115,250 calendar years BP. Phenocrysts are the main phase comprising K-
361 feldspar, zoned plagioclase, light-greenish clinopyroxene, orthopyroxene and olivine. In
362 addition, rare lithic clasts of quenched feldspar crystals and tachylites occur. The juvenile
363 phase is made up of greyish-brownish, non- to low-vesicular volcanic glass that exhibits a
364 rather heterogeneous calc-alkaline, trachyandesitic composition that is typical for magmas
365 erupting from several of the Aeolian Islands. Glass shards of TM-32 show SiO₂
366 concentrations of ca. 60 wt%, high FeO values of about 6.5 wt%, and concentrations of CaO,
367 Na₂O and K₂O of about 4-5 wt%, respectively. A comparison with glass data of the 85.3 ka
368 BP Petrazza Pyroclastic Series and the equivalent distal tephra TM-21 (Wulf et al., 2004)

369 show some similarities suggesting Stromboli volcano as a potential source, though TM-32
370 shows higher FeO and K₂O but lower SiO₂ concentrations (Fig. 4d). However, no Stromboli
371 activity in the considered time period is known (Hornig-Kjarsgaard et al., 1993; Gillot and
372 Keller, 1993), thus leaving a precise correlation of TM-32 open.

373

374 *Please place here Figure 4c and Figure 4d.*

375

376 **TM-33** comprises two depositional units, TM-33-1 and TM-33-2, with a set of several tephra
377 layers of similar composition. Tephra unit TM-33-1 is made up of three light-brownish, vitric
378 ash layers up to 11 mm in thickness, deposited in 83.05 to 83.10 m composite depth. These
379 layers are dated by the Monticchio chronology between 115,720 and 116,110 calendar years
380 BP. Tephra unit TM-33-2 comprises two thin tephra layers in ca. 83.43 m composite depth,
381 which are dated at 118,190 and 118,210 calendar years BP, respectively. Tephra TM-33-1
382 and TM-33-2 all consist of abundant light-brownish, medium- to high-vesicular pumice
383 fragments and few large sanidine, plagioclase, biotite and rare clinopyroxene (Aegerine-
384 augite) phenocrysts. Scarce lithics comprise clasts of quenched crystals and sedimentary rock
385 fragments (sandstones, siltstones). Glass shards of each tephra unit show a bimodal trachytic
386 composition (Fig. 4e). The major element chemistry within each unit differs in the
387 concentration of SiO₂ (60.8–63.1 wt%) and CaO (1.0–2.1 wt%). The K₂O/Na₂O ratios show
388 values of 0.8 and 1.4 for the lower and the upper tephra layers, respectively. In summary, the
389 chemical composition of most tephra of unit TM-33 resembles that of Ischia pyroclastics
390 (Fig. 4e). A tentative correlation can be made on the basis of the chronostratigraphical
391 position of Monticchio tephra layers. Accordingly, units TM-33-1 and TM-33-2 most likely
392 relate to the Punta Imperatore Formation dated at ca. 118.5 ka BP (K/Ar weighted mean age;
393 Gillot et al., 1982; Vezzoli, 1988).

394

395 **TM-34** is a distinct 0.4 mm thin tephra layer in 83.54 m composite depth that is dated at
396 118,810 calendar years BP. This fine-grained ash consists of blocky, non- to low-vesicular
397 brown glass shards bearing apatite microcrystals. Phenocrysts comprise the minerals
398 plagioclase and pale-greenish clinopyroxene with adherent glass. Few lavic lithics also occur.
399 Volcanic glasses are heterogeneous Na-calcalkaline, trachyandesitic to basaltic
400 trachyandesitic in composition, showing strong variations in SiO₂ (54.4–57.8 wt%) as well as
401 high FeO (8.4–11.3 wt%), MgO (2.4–3.8 wt%) and CaO (6.2–8.2 wt%) concentrations. The
402 comparison of published major element data of pyroclastics and lava products strongly

403 suggest an origin of TM-34 from the Aeolian Islands (Fig. 4f). Explosive volcanism during
404 the considered time interval is particularly known from the Islands of Salina and Lipari. On
405 Lipari, on the one hand, the Monte San Angelo center was explosively active between 127 ± 8
406 ka BP and 92 ± 10 ka BP (Esperança et al., 1992), and erupted pyroclastics of the related
407 cycles III and IV of Lipari are chemically (bulk samples) similar to TM-34 (Fig. 4f). The
408 Fossa delle Felci stratovolcanic center on Salina, on the other hand, produced several sub-
409 Plinian to strombolian fallout deposits within two distinct eruptive sequences of older basaltic
410 (127 ± 5 ka BP, K/Ar; Gillot, 1987; Gertisser and Keller, 2000) and younger andesitic to
411 dacitic volcanics (Keller, 1980; Gertisser and Keller, 2000). The latter comprise pyroclastics
412 of the stages 5-8 showing a bulk composition that approximates most the glass composition of
413 tephra TM-34. Volcanism of the Fossa delle Felci is supposed to have lasted no longer than a
414 few ten thousand years (Gertisser and Keller, 2000) and therefore the age of its younger
415 products (<127 ka BP) is well in the time frame of the deposition of TM-34 in Monticchio.
416 The best chemical match of glass data, however, is given by a secondary glass component of a
417 coarse-grained turbidite found in Marsili Basin core TIR2000-398 cm from the Tyrrhenian
418 Sea (Fig. 4f) (Albert et al., 2012). These components are tentatively interpreted to represent
419 older, so far undated activity of Salina that was incorporated during a younger collapse of the
420 island. In summary, a reliable correlation of tephra TM-34 with a dated proximal counterpart
421 is not possible at this moment, but the source can be most likely narrowed down to Salina
422 Island.

423

424 *Please place here Figure 4e and Figure 4f.*

425

426 **TM-35** comprises two tephra layers of similar composition, TM-35a (120,670 calendar years
427 BP) and TM-35b (121,940 calendar years BP) in 84.14 m and 84.84 m composite depth,
428 respectively. Both tephtras consist of light, high-vesicular pumice fragments and large
429 phenocrysts of sanidine, plagioclase, biotite and rare green clinopyroxene. Lithics comprise
430 clasts of quenched crystals and altered tuffs. Geochemical data are only available for the more
431 coarse-grained tephra TM-35a. Those reveal a homogeneous trachytic composition with CaO
432 concentrations of about 2 wt% and K_2O/Na_2O ratios of ~ 1.5 (Fig. 4a). The composition
433 suggests a general origin of tephtras TM-35 from a so far unknown eruption of the Campanian
434 Volcanic Province.

435

436 **TM-36** is a fine-grained, brown-blackish ash layer in 85.30 m composite depth, which is
437 dated at 123,030 calendar years BP. It contains light, high-vesicular pumice fragments,
438 abundant large phenocrysts of sanidine, leucite, nepheline, biotite, apatite and green
439 clinopyroxene, as well as rare altered tuffs and limestone fragments. Tephra components are
440 set in a black (base) and brown (top) fine-grained matrix. Glass shards show a phonolitic
441 composition with high Al₂O₃ values of 20.3 – 20.8 wt% and CaO concentrations of 4.1 – 5.3
442 wt%. This chemical composition is typical for products from the Sabatini Volcanic District
443 (Roman Province) (Fig. 4g), which we consider as the source area for TM-36. The last
444 activities of the Sabatini Volcanic District produced a cluster of dominantly hydromagmatic
445 and subordinate magmatic eruptions of similar phonolitic composition (Sottili et al., 2010;
446 Sottili et al., 2012). A good geochemical match, for instance, is given by the Upper
447 Stracciaccappa unit (Fig. 4g), though this unit is significantly younger (97 ± 4 ka BP; Sottili et
448 al., 2012) than the varve age obtained for tephra TM-36. The Baccano Lower Unit, described
449 as a leucite/analcime bearing white pumice fall deposit, erupted rather in the considered time
450 period (131 ± 2 ka BP; Sottili et al., 2012), but has not been geochemically characterized, so
451 far. The closest chemical and chronological match is given by the pyroclastics of the Valle dei
452 Preti unit (VdP; Sottili et al., 2012) (Fig. 4g). The VdP unit was formerly dated at $>296 \pm 3$ ka
453 BP (Sottili et al., 2012). New stratigraphical data, however, indicate a much younger
454 formation age that is closer to the considered time frame of the deposition of tephra TM-36
455 (i.e., younger than the Cornacchia Lava dated at 154 ± 7 ka BP; (Nappi and Mattioli, 2003). A
456 detailed correlation, however, requires more analytical data of proximal pyroclasts, which are
457 in progress.

458

459 *Please place here Figure 4g.*

460

461 **TM-37** is a succession of four single tephra layers deposited between 85.68 m and 86.59 m
462 composite depth. Layer thicknesses range between 1 mm and 1.1 cm (Table 1). The oldest
463 tephra TM-37d (124,860 calendar years BP) is a white, fine-grained, almost pure vitric ash
464 with high-vesicular glass components. It is overlain by pumice fallout TM-37c (124,360
465 calendar years BP) that is abundant in rock fragments (clasts with quenched crystal, lavic
466 lithics, and altered green tuffs with feldspar xenocrystals) and phenocrysts of sanidine,
467 plagioclase, biotite, green clinopyroxene and amphibole. Here, high-vesicular white pumice
468 clasts and rare brown glass shards are common. The slightly younger tephra TM-37b (124,330
469 calendar years BP) is similar in composition but thicker and more coarse-grained than TM-

470 37c and TM-37d. The most prominent tephra layer is the youngest and thickest deposit TM-
471 37a (124,070 calendar years BP). It is twice reversely graded and mainly composed of high-
472 vesicular white pumice fragments. Abundant phenocrysts and lithics comparable with those in
473 layers TM-37b and TM-37c occur at the base of the deposit. All tephra layers of succession
474 TM-37 are homogeneous trachytic in composition showing low CaO concentrations (1.0–1.3
475 wt%) and K₂O/Na₂O ratios between 0.8 and 1.0. Tephra of this composition are typical for
476 Ischia eruptions (Fig. 4e). For the proposed time of deposition between 124 and 125 ka BP,
477 however, volcanic activity on Ischia was restricted to the formation of lava domes and minor
478 lava flows from the Castello d'Ischia and Monte di Vezzi volcanic centres (126 ± 4 ka BP;
479 K/Ar; Gillot et al., 1982). It is speculative whether these activities were accompanied by the
480 eruption of larger amount of tephra material, and therefore a correlation of tephra TM-37
481 with proximal pyroclastic deposits remains open for now.

482

483 **TM-38** (formerly labelled as TM-38a in Wulf et al., 2006) is a fine-grained, vitric ash in
484 87.07 m composite depth. It is composed of light-coloured glass shards of homogeneous high-
485 K-phonolitic composition (Fig. 4a). A few loose crystals of sanidine and biotite also occur.
486 Tephra TM-38 is dated by the Monticchio chronology at 125,550 calendar years BP and most
487 likely originates from an unknown eruption of the Campanian Volcanic District.

488

489 **TM-39** is a brownish tephra layer of 4 mm thickness at 91.98 m composite depth. It
490 comprises brown and minor light low- to moderate-vesicular glass shards of similar
491 homogeneous phonolitic composition that exhibit higher FeO (4.5 wt%) and CaO (3.3 wt%)
492 concentrations and lower K₂O/Na₂O ratios (1.3–1.7) than tephra TM-38 (Fig. 4a). Phenocrysts
493 encompass the minerals plagioclase, sanidine, green clinopyroxene, and amphibole. Leucite
494 and apatite microcrystals occur as well as lithics of lavic rocks. TM-39 is dated at 130,530
495 calendar years BP. According to its chemical composition it most likely originates from a
496 Campanian volcano.

497

498 **TM-40** in 92.37 m composite depth is a white vitric ash of 5 mm thickness. It bears
499 phenocrysts of sanidine, biotite and greenish clinopyroxene. Lithics are rare and comprise
500 clasts of quenched crystals. The main juvenile phase is characterized by light high-vesicular
501 and few brownish glass shards of inhomogeneous trachytic composition. The K₂O/Na₂O ratio
502 of ~1 as well as variable CaO concentrations between 1.2 and 2.2 wt% (Fig. 4e) indicate an
503 origin of TM-40 from a Campanian volcano with Ischia as a potential source volcano.

504

505 **TM-41** (formerly labelled as TM-38b in Wulf et al., 2006) is a double layered, light brownish
506 tephra of 6 mm thickness. It occurs at 92.77 m composite depth and is dated at 131,020
507 calendar years BP. Glass shards are light to brownish in colour and low-vesicular. The glass
508 composition is heterogeneous trachytic to phonolitic, reflecting variable concentration of CaO
509 (1.5-3.1 wt%), FeO (1.2-3.5 wt%), K₂O/Na₂O ratios (1.4-2.4) and high Al₂O₃ values (19.3–
510 21.0 wt%) (Fig. 4e). The mineral assemblage encompasses phenocrysts of sanidine,
511 plagioclase, biotite, clinopyroxene and apatite microcrystals. Rare volcanic rock fragments
512 and clasts of quenched crystals also occur. The maximum grain sizes of 300 µm in
513 combination with the composition strongly suggest an origin from a Campanian volcano.

514

515 **TM-42** is a 1 mm thick light ash in 97.69 m composite depth. It is the oldest tephra layer in
516 the Monticchio record dated at 132,110 calendar years BP. The mineral assemblage is
517 composed of sanidine, plagioclase, biotite and minor green clinopyroxene crystals. Lithics are
518 rare and comprise clasts of quenched crystals of intermediate composition. The juvenile phase
519 is made up of light high-vesicular pumice fragments of homogenous trachytic character,
520 which is typical for Ischia products (Fig. 4e). Based on its composition and age constraints we
521 propose a tentative correlation of TM-42 with the Lower Scarrupata di Barano Formation
522 ($>123 \pm 3.4$ ka BP, K/Ar; Gillot et al., 1982).

523

524 *Please place here Table 3.*

525

526 **6 Discussions**

527 **6.1 Tephra sources and distal correlation**

528 The extended Monticchio tephra record, now reaching back to 133 ka BP, provides a total
529 number of 345 visible and primary (non-reworked) tephra fallout layers. Out of these, 293
530 tephra layers were described from the upper ≤ 100 ka BB section (Wulf et al., 2004; Wulf et
531 al., 2006; Wulf et al., 2008) and 52 tephtras are identified in the extended sediment section
532 between 72.5 and 103.1 m, covering the interval from 100 ka BP to 133 ka BP. Major-
533 element glass data in combination with microscopic-petrographic results suggest sources of
534 these older ashes within the Campanian, Roman and Sicilian-Aeolian volcanic provinces in
535 central and southern Italy. Detailed correlations with proximal deposits, however, are quite
536 difficult mainly due to the lack of comparable geochemical and/or chronological data of
537 potential correlatives. Chemical comparisons are mainly based on published XRF whole rock

538 data of pyroclastic and lava material. Whole rock analyses may significantly differ from
539 grain-specific EPMA and SEM-EDS glass analyses, which is particularly dependent on the
540 proportions of phenocrysts present within the tephra deposit. Such differences are known, for
541 instance, from the younger tephra deposits of Mount Etna, the widespread Biancavilla/Y-1
542 tephra (17.3 ka BP), which shows a wide range in SiO₂ concentration of glass shards (60-66
543 wt%) compared to the respective whole rock data (~60 wt%; Coltelli et al., 2000) (Fig. 4b). A
544 similar behaviour is expected for older Etnean tephra deposits of the AAC. In contrast, other
545 volcanic centres such as Ischia Island exhibit only minor or none compositional differences
546 between bulk composition and single-grain glass data. Here, the problem of a reliable
547 correlation with distinct older proximal deposits lies in the similarity of erupted tephtras.
548 Consequently, a clear discrimination of individual layers is not possible, and tentative
549 correlations are almost solely based on chronological and stratigraphical information.
550 Problems in respect to reliable correlations are also given for more “exotic” tephtras deriving
551 from Roman and Aeolian Islands volcanoes. Here, the glass chemical compositions of tephtras
552 clearly refer to their respective provenances, but reliable correlations are difficult due to the
553 lack of either one or both chemical and chronological-stratigraphical data of proximal tephra
554 deposits.

555 The only strong correlations of Monticchio tephtras, however, are given from other distal
556 terrestrial or marine equivalents, which are independently dated either by K/Ar and Ar/Ar
557 methods or by orbital tuning of oxygen isotope records of foraminifera in deep-sea sediments.
558 Juvenile glass components are chemically characterized by either EPMA or SEM-EDS
559 techniques. Those correlations, however, are restricted to only a few widespread marker
560 layers in the Central Mediterranean (i.e., Keller et al., 1978; Munno and Petrosini, 2007;
561 Marciano et al., 2008; Paterne et al., 2008).

562

563 **6.1.1 Tephtras from Ischia Island**

564 During the last 133 kyrs numerous larger pyroclastic units erupted from the Island of Ischia.
565 An example for the high intensity of explosive eruptions is given by the Y-7 / IT (“Ischia
566 Tephra”) that was recognized as a prominent and widespread marker in the land and deep-sea
567 records of the Central Mediterranean (Keller et al., 1978; Morche, 1988; Gillot and Keller,
568 1993; Keller and Kraml, 2004; Lucchi et al., 2008) and dated at 56 ± 4 ka BP (Kraml, 1997;
569 Keller and Kraml, 2004). In the time span 100-133 ka, three pyroclastic fall deposits - the
570 Punta Imperatore, the Upper (USB) and Lower Scarrupata di Barano (LSB) Formations - are
571 recognized in proximal sites from Ischia Island (Vezzoli, 1988). These explosive phases are

572 accompanied by lava dome and flow activities of the Monte di Vezzi / Castello d'Ischia,
573 Rione Bocca and Monte Cotto / La Guardiola volcanic centres (Vezzoli, 1988). A wide and
574 overlapping range of ages is given for most of the Ischia volcanic units mainly due to the use
575 of different dating material such as whole rock material, groundmass and sanidine crystals
576 (Gillot et al., 1982; Poli et al., 1989; Vezzoli, 1988). The only consistent age constraint,
577 however, is provided for the Punta Imperatore Formation (116 ± 2.6 ka BP to 123 ± 2.7 ka
578 BP; Gillot et al., 1982). This timing in combination with geochemical evidence (Fig. 4e)
579 provides the only reliable Ischia correlation marker for tephra successions TM-33 (ca. 118.2–
580 115.7 ka BP) in the Monticchio record. For the older Ischia tephtras TM-40 (130.9 ka BP) and
581 TM-41 (131 ka BP), it can be only speculated whether the heterogeneity of major element
582 glass composition is comparable with the bimodal bulk lava composition provided by
583 different methods for the USB Formation (Fig. 4e). Consequently, the younger tephtras TM-37
584 (ca. 124.9–124.1 ka BP) may be related to yet unrecognized pyroclastic activities between the
585 Punta Imperatore and USB formations, that may have occurred, for instance, at the Monte di
586 Vezzi volcanic centre (126 ± 4 ka; Gillot et al., 1982). Though the geochemical signature of
587 TM-37 approximates the bulk composition of the Monte di Vezzi lava flow (Fig. 4e),
588 evidence for coeval tephra emission is still missing and therefore only vague statements of a
589 potential correlation with the Monte di Vezzi lava flow activities are possible. In respect to
590 the oldest Ischia tephra TM-42 (ca. 132.1 ka BP), geochemical similarities occur with bulk
591 data of pumices from the LSB Formation (Fig. 4e). The dating of the LSB, however, appears
592 problematic. The only time constraints derive from K/Ar dates of the overlying Monte Cotto
593 and La Guardiola lavas that propose minimum ages of the LSB between 123 ± 3.4 ka BP
594 (Sanidine) and 147 ± 3 ka BP (groundmass) (Vezzoli, 1988). The wide age range and the lack
595 of comparable EPMA glass data hence provide only an ambiguous correlation of tephra TM-
596 42 with proximal deposits on Ischia Island.

597 Distal tephtras from Ischia older than 105 ka BP are also recorded in sediment cores
598 from the Central Tyrrhenian and Ionian Seas (Paterne et al., 2008) (Table 3). Tephra C-35
599 found in 485 cm sediment depth in Ionian Sea core KET 82-22 and dated at 121.5 ka BP, was
600 tentatively assigned to the 108-110 ka marine X-6 tephra (Paterne et al., 2008). Another
601 marine tephra, C-34, in Tyrrhenian Sea core DED 87-08 in 1260 cm and an overlying mixed
602 (reworked?) tephra layer in 1254 cm sediment depth dated at 116.1 ka and 115.2 ka BP,
603 respectively, show a similar glass composition. The SEM-EDS glass composition of both C-
604 34 and C-35 match the EPMA composition and the age of the Monticchio tephra layer
605 sequence TM-33 (116-118 ka BP; Punta Imperatore Formation) (Table 3, Fig. 4e). Tephtras

606 TM-40 (130.9 ka BP) and TM-41 (131 ka BP) show as well some minor affinities to tephras
607 C-34 and C-35, but most likely derive from a different Campanian source volcano due to the
608 high CaO concentrations of >2 wt% (Fig. 4e). In respect to Monticchio tephras TM-37 and
609 TM-42, distal correlative have not been identified so far.

610

611 **6.1.2 Tephras from unknown Campanian sources (Phlegrean Fields?)**

612 36 tephra layers in the Monticchio record clustering around 105.8–114.7 ka and 121–131.3 ka
613 BP show a K-phonotrachytic glass composition that is typical for more recent tephra products
614 erupted from Campanian volcanoes, and more precisely from the Phlegrean Field caldera. The
615 youngest tephra TM-25 of generic Campanian origin densely clusters within the chemical
616 fields of the marine X-5 tephra. The prominent pair of X-5 and X-6 tephra layers, as defined
617 in the Ionian Sea by Keller et al. (1978) occupies a well-defined position between the Ionian
618 sapropels S4 and S5. The varve age of Monticchio tephra TM-25 is ca. 105.8 ka BP, which is
619 in close agreement with the $^{40}\text{Ar}/^{39}\text{Ar}$ age of 105 ± 2 ka BP obtained on the marine X-5 tephra
620 by Kraml (1997). TM-25 geochemically and chronologically also matches the C-27 tephra
621 layer (103.5 ka BP) in the Tyrrhenian Sea cores DED 87-08/KET 80-04 (Paterne et al., 2008)
622 and the POP3 layer (106.2 ± 1.3 ka BP; $^{40}\text{Ar}/^{39}\text{Ar}$) from a central Italy lacustrine succession
623 (Popoli, Sulmona Basin; Giaccio et al., submitted) (Fig. 4a). Marine tephras X-5 and C-27
624 were originally assigned to the two distinct Monticchio tephras TM-24a (ca. 101.8 ka BP) and
625 TM-24b (ca. 102.8 ka BP) in the Monticchio record based on initial major and trace element
626 data (Wulf et al., 2004). Additional major element glass data obtained on TM-24a and TM-
627 24b (Fig. 4a) prove a wider range in glass composition and therefore differ from the rather
628 homogenous X-5 and TM-27 glass compositions. Also maximum grain sizes of pumices in
629 tephras TM-24a and TM-24b are smaller than in TM-25 indicating a lower magnitude
630 eruption for the TM-24 couplet compared to the widespread TM-25/X-5 eruption.

631 The thickest Monticchio tephra TM-27 (ca. 108.3 ka BP) matches the widespread
632 marine X-6 tephra at ca. 108-110 ka BP (Keller et al., 1978; Kraml, 1997; Keller and Kraml,
633 2004) and therefore forms an important regional tephrochronological synchronisation marker.
634 Furthermore, the comparison of single grain glass data shows that TM-27/X-6 can be
635 attributed to the marine C-31 tephra (107 ka BP) that forms a thick and coarse grained marker
636 layer in sediment cores KET 80-04, DED 87-08 and KET 82-22 in the Central Tyrrhenian and
637 Ionian Seas (Paterne et al., 2008) (Table 3). Noteworthy, the TM-27/X-6 tephra in the
638 Monticchio sequence is preceded by two thin and fine-grained layers, TM-28a and TM-28b,
639 which are chemically almost identical to TM-27. These tephras are approximately 2000 and

640 2500 calendar years older and probably derive from the same unidentified Campanian
641 volcanic source.

642 The second older cluster of Monticchio tephra deriving from not well-defined
643 Campanian sources comprises tephra units TM-29 and TM-30 as well as tephra layers TM-31,
644 TM-35, TM-38 and TM-39. Out of those, the compositionally highly variable tephra layers of
645 succession TM-29, TM-30 and TM-31 (111.5-114.7 ka BP) match the glass composition of
646 tephra OT0701-7 from a sediment sequence of Lake Ohrid, Balkans (Fig. 1a) correlated with
647 the TAU1-b tephra deposit of the Campanian area (Sulpizio et al., 2010). In addition, one
648 glass component occurring in a mixed tephra layer in 1254 cm sediment depth in Tyrrhenian
649 Sea core DED 87-08 and dated at 115.2 ka BP shows a similar composition as glass shards
650 from Monticchio tephra layer TM-29-1g (Table 3, Fig. 4c) indicating the same source.

651 The high-K trachytic Monticchio tephra TM-35a (ca. 120.7 ka BP), in turn, is
652 approximating the glass composition of a distal tephra in the marine realm, the C-36 tephra
653 layer in Tyrrhenian Sea core KET 80-04 (123.2 ka BP; Paterne et al., 2008) (Fig. 4a, Table 3).
654 For Monticchio tephra TM-38 and TM-39 neither proximal nor distal tephra equivalents were
655 identified, so far.

656 Though the lack of a complete chronological and EPMA geochemical dataset hampers
657 a precise correlation, Monticchio tephra of Campanian provenance can be most likely
658 associated with compositionally similar pyroclastic units recognised in the Neapolitan area,
659 dated between 125 ka and 39 ka BP (Di Vito et al., 2008). Based on field evidence these units
660 were tentatively attributed to early, unknown explosive activities localised in the Phlegrean
661 Fields area (Di Vito et al., 2008).

662

663 **6.1.3 Tephra from Mount Etna and the Aeolian Islands**

664 The most remarkable Monticchio tephra in terms of their geochemical composition are
665 tephra TM-26, TM-32 and TM-34. These ashes can be related to early pyroclastic activities
666 of Mount Etna and the Aeolian Islands. The lack of exposure and/or glass compositional data
667 of proximal deposits and distal occurrences, however, only allows tentative correlations that
668 are based on general geochemical signatures of products of source volcanoes described in
669 literature. This applies in particular to tephra TM-26 (Mount Etna, ca. 106.3 ka BP) and TM-
670 32 (Stromboli, ca. 115.2 ka BP) that show chemical affinities to younger tephra of the
671 respective volcanoes. Apart from XRF whole rock data of proximal pyroclastics, tephra TM-
672 26 can only be compared with SEM-EDS glass data of Etnean origin found in 1093-1095 cm
673 and 1139-1141 cm sediment depth in Tyrrhenian Sea core KET 80-04 (Table 3). Those distal

674 shards dated at 124.6 ka and 130.2 ka BP, respectively, are significantly older than TM-26,
675 but are similar in composition and therefore confirm the considered correlation with older
676 Etnean deposits. Tephra TM-32 shows strong affinities to Paleostromboli I pyroclastics, but
677 neither entirely matches the glass composition nor fits the age of the 75.3 ka BP Petrazza
678 pyroclastic series, the oldest pyroclastics found on Stromboli so far (Hornig-Kjarsgaard et al.,
679 1993). Tephra TM-34 (ca. 118.8 ka BP) can be associated with Salina Island pyroclastics, and
680 matches best the composition of glass shards found in a turbidite from a Marsili Basin core
681 (Albert et al., 2012). Both, TM-32 and TM-34 are not documented as discrete primary tephra
682 layers in other environments yet, and therefore a detailed correlation with independently dated
683 events remains open.

684

685 **6.1.4 Tephra from Roman volcanoes (Sabatini Volcanic District)**

686 Out of the 52 primary tephra fallout layers, only one single tephra layer in the Monticchio
687 sediment section, tephra TM-36 (ca. 123 ka), can be attributed to Roman volcanic activities.
688 Tephra TM-36 shows strong affinities to late stage pyroclastics of the Sabatini Volcanic
689 District. Those activities were characterized by the formation of maars such as the Valle dei
690 Preti, Stracciacappa, Le Cese, Acquarella and Martignano (Sottili et al., 2012). The related
691 proximal pyroclastic deposits are well studied (Sottili et al., 2012) and provide valuable
692 EPMA data for the comparison of major-elements with TM-36 (Table 3). Here, the best
693 chemical and chronological fit is given for the Valle dei Preti Units ($<154 \pm 7$ ka BP) (Fig.
694 4g). Distal equivalents of tephra TM-36 were not found as distinct layers elsewhere so far. In
695 Tyrrhenian Sea core DED 87-08, 1254 cm sediment depth, however, a mix of volcanic glass
696 of different composition exposes also a phonolitic component that is comparable with TM-36
697 (Table 3, Fig. 4g). This marine tephra layer, however, is dated at 115.2 ka BP and therefore
698 considerably younger than TM-36.

699

700 *Please place here Table 5.*

701

702 **6.2 Revising tephrochronology**

703 The revision of the varve and sedimentation rate chronology of the Monticchio sediments
704 (Brauer et al., 2007) lead to changes of the timing of tephra deposited prior to the TM-
705 13/Pomici di Base eruption (19,280 calendar years BP; Wulf et al., 2004). As a result, tephra
706 ages became systematically older, i.e. the TM-15/Y-3 tephra now dates at 27,260 instead of
707 23,930 calendar years BP, whereas the timing of the TM-18/Campanian Ignimbrite tephra

708 layer is corrected to an older age of 36,770 calendar years BP. A complete list of revised ages
709 of main tephra markers defined in Wulf et al. (2004) is provided in Table 4. Those dates in
710 addition to three new varve dates resulting from the extended Monticchio 100-133 ka BP
711 section are used to re-built a tephrochronological framework, which is then compared with
712 updated radiometric and radioisotopic ages (weighted mean ages with 2σ error range) of
713 correlated counterparts obtained from other proximal and distal records elsewhere (Fig. 5,
714 Table 4). The juxtaposition of both chronologies shows a general good agreement, though in
715 some sections large and variable uncertainties are noticeable:

- 716 ▪ **Section 1** (0–1.15 m composite depth): Sediments of the topmost 50 cm are homogenous
717 and the lamination is not well preserved. The varve age of tephra TM-1/AD 1631 in 6 cm
718 depth is estimated too young, most likely indicating missing sediments in the top section.
719 Sediments in the lower section, in turn, are laminated (organic varves). Here, the calendar
720 ages of tephras TM-2a/AD 512 and TM-2b/AD 472 Pollena agree well with a 2%
721 uncertainty with the historical documented ages of tephra events.
- 722 ▪ **Section 2** (1.15–10.15 m composite depth): Approximately 90% of the Monticchio
723 sediments in this section between 1,500 and 18,000 calendar years BP are annually
724 laminated (organic varves). The varve age of the TM-4/Avellino tephra of 4,310 calendar
725 years BP in the upper part is within the 2σ error range of radiocarbon ages obtained in
726 proximal and distal deposits (Table 3), but shows an older age with a difference of 9.2%
727 compared to the weighted mean radiometric age of correlated equivalents. Varve ages of
728 the directly overlaying tephras TM-3b/AP3 (4,020 calendar years BP) and TM-3c/AP2
729 (4,150 calendar years BP), in turn, are significant older than the respective ^{14}C ages of
730 proximal correlatives (41% and 19.7% uncertainty). However, based on the good
731 preservation of varves in the section between ca. 3,500 and 4,500 calendar years BP large
732 varve counting errors and/or a hiatus can be excluded suggesting rather an overestimation
733 of varves in the younger sediment section (1,500-3,500 calendar years BP). Monticchio
734 varve ages of the TM-4/Avellino underlying tephras TM-5a/Agnano Mt. Spina, TM-
735 7/Pomici Principali, TM-8/Neapolitan Yellow Tuff, TM-9/GM1 and TM-10d/Lagno
736 Amendolare (4,620–15,550 calendar years BP) are in good agreement with ^{14}C and
737 $^{39}\text{Ar}/^{40}\text{Ar}$ ages of correlatives with a mean uncertainty of 3.4%. The TM-6b/Mercato
738 tephra (9,680 calendar years BP) is the only outlier, showing an older varve age in respect
739 to the radiometric dating (8.7% uncertainty). In the lowermost section (9.5-10.15 m), the
740 ages of the TM-11/Biancavilla tephra (16,440 calendar years BP) and the TM-
741 12/Verdoline tephra (17,560 calendar years BP) appear too young, and a systematic

742 increase of deviation up to 7.2% (ca. 1360 years) between varve and radiometric ages of
743 tephra is notable. This difference is most likely based on an underestimation of varves in
744 this section of poor varve preservation.

745 ■ **Section 3** (10.15–18.00 m composite depth): Below the TM-12/Verdoline tephra, the
746 annual lamination of the organic-clastic sediments is poorly preserved and therefore likely
747 leads to an underestimation of varves. Age uncertainties increase to an average of 10%
748 which corresponds to 2420 years for the TM-13/Pomici di Base tephra (19,280 calendar
749 years BP) and up to ca. 4000 years for the TM-17bc/Albano unit 7 tephra (31,830 calendar
750 years BP). Marker tephra TM-14/Solchiaro and TM-16b/Codola are re-dated to 21,260
751 and 31,120 calendar years BP, respectively.

752 ■ **Section 4** (18.00–27.00 m composite depth): The annual lamination of the minerogenic-
753 calcareous sediments is exceptionally well preserved in the new cores LGM-M and LGM-
754 O between tephra TM-17bc/Albano unit 7 and TM-18/Campanian Ignimbrite, and
755 therefore has been re-counted (Funk, 2004). As a result, the new varve age of 36,770
756 calendar years BP for the TM-18/Campanian Ignimbrite tephra is now well within the 2σ
757 error range of three radiometric and five $^{40}\text{Ar}/^{39}\text{Ar}$ dates of proximal and distal
758 correlatives and shows an uncertainty of ca. 6% in respect to the weighted mean age
759 (Table 4).

760 ■ **Section 5** (27.00–60.00 m composite depth): The section between 37,000 and 90,000
761 calendar years BP (MIS 3 to 5b) exhibits organic-minerogenic sediments that are poorly
762 laminated with an exception between 50 and 58 m sediment depth (76,000–88,000
763 calendar years BP, MIS 5a). Major tephra markers occur in the lower part between 40 and
764 60 m and include TM-19/TVEss, TM-20/UMSA, TM-21/Petrazza and TM-22/Ignimbrite
765 Z. The two Ischia tephra layers TM-19/TVEss and TM-20/UMSA are re-dated in the
766 Monticchio sediments from previously 56,250 and 57,570 calendar years BP to 60,060
767 and 61,370 calendar years BP, respectively. The new varve ages, however, appear too old,
768 though they are still within the 2σ error range of $^{39}\text{Ar}/^{40}\text{Ar}$ and K/Ar ages obtained on
769 proximal and distal correlatives. This assumption is supported by the varve age of the
770 preceding TM-21/Petrazza tephra (78,340 calendar years BP), which is 3100 years older
771 than the K/Ar age of 75.3 ka BP (Gillot and Keller, 1993) of its proximal correlative. The
772 varve age of tephra TM-22 (Ignimbrite Z of Pantelleria, marine tephra layer P-10) is
773 corrected from previously 85,320 to 89,130 calendar years BP, and is now 5000 years
774 older than the marine oxygen isotope age of the distal equivalent. In total, the mean age
775 uncertainty is approximately 7% indicating an overestimation of varve ages in this section.

- 776 ▪ **Section 6** (60.00–70.20 m composite depth): The section between 90,000 and 101,000
777 calendar years BP (MIS 5b/5c) constitutes minerogenic-organic sediments that are more
778 or less well laminated in the upper 70% of the succession. In the lower part, varve
779 preservation is poor. Though a total of 81 tephra fallout layers occur in this section, only
780 one tephra could be assigned to a dated correlative. The trachytic tephra TM-23-11 was
781 recently matched with the terrestrial POP1 tephra occurring in the Popoli section,
782 Sulmona Basin (Latium) and dated by $^{40}\text{Ar}/^{39}\text{Ar}$ at 92.4 ± 4.6 ka BP (Giaccio et al.,
783 submitted). Here, the Monticchio varve age of 95,180 calendar years BP is well within the
784 2σ error range, but ca. 3000 years older than the mean radioisotopic age of its correlative
785 indicating an overestimation of varves with an age uncertainty of ca. 3.2% in this section.
- 786 ▪ **Section 7** (70.20–92.50 m composite depth): The newly studied section between 101,000
787 and 131,000 calendar years BP is well laminated, showing a variety of varve types of
788 organic-minerogenic (MIS 5c), organic (MIS 5e) and calcareous-minerogenic (MIS 6)
789 composition. Prominent tephra marker layers such as TM-25/X-5 and TM-27/X-6 occur in
790 the upper part of this section providing valuable dating points at 105,480 and 108,330
791 calendar years BP. These are in very good agreement (0.3 and 0.5% uncertainty) with the
792 dates obtained from the marine equivalents (Table 4). This implies an underestimation of
793 varve ages in the poorly laminated section 6. In the lower part of section 7, the tentative
794 correlation of the TM-33 succession (118,210 calendar years BP) with the Punta
795 Imperatore Formation confirms the Monticchio chronology with an even lower
796 uncertainty of ca. 0.1%.
- 797 ▪ **Section 8** (92.50–103.10 m composite depth): The basal part of the Monticchio record is
798 characterized by the deposition of a large number of turbidites formed during the early
799 phase of lake development. So far, no robust time control is given for the sediments older
800 than 131,000 calendar years BP, though an underestimation of varves of at least 10% is
801 possible (Brauer et al., 2007).

802

803 *Please place here Figure 5.*

804

805 **6. Conclusions**

806 The Monticchio tephra record exhibits 345 visible tephra fallout layers that are distributed
807 throughout the last 133 kyrs and precisely dated by the revised varve supported sedimentation
808 rate chronology of Monticchio sediments (Brauer et al., 2007). This chronology is confirmed
809 independently by 28 radiometric and radioisotopic ages of prominent tephra correlatives with

810 a mean age uncertainty of 5%. Revised varve ages are provided for all Monticchio tephras
811 >19,280 calendar years BP; i.e., the new age estimate for the Campanian Ignimbrite tephra
812 fall (TM-18 / CI / Y-5) now has a varve age of $36,770 \pm 1840$ calendar years BP (2σ error),
813 which is still too young but closer to the widely accepted $^{40}\text{Ar}/^{39}\text{Ar}$ date of 39.28 ± 0.11 ka BP
814 obtained by De Vivo et al. (2001).

815 The detailed study of the 52 newly identified tephras between 100 and 133 ka BP allows
816 defining sources in the southern and central Italian volcanic area. Most of these ashes were
817 not described elsewhere, so far. Therefore, reliable assignments to single eruptive events were
818 possible on a limited basis only. Those were the correlations with the prominent marine
819 tephras X-5 (ca. 105 ka BP) and X-6 (ca. 107 ka BP) which are varve dated with an
820 uncertainty of less than 1% (Brauer et al., 2007). Other less well constrained correlations are
821 based either on age constraints or tentative geochemical matches. This brings up three main
822 issues that need to be resolved by the tephra community in the future:

- 823 1. The description of tephra deposits, particularly in proximal sites, often lacks in EPMA
824 glass data. These data, however, are essential for reliably correlating distal findings
825 and should thus be provided for all ash layers in any type of archive.
- 826 2. Detailed chronological constraints of tephras are well derived for major eruptive
827 events like, for example, the Avellino (4 ka BP), Neapolitan Yellow Tuff (14 ka BP)
828 and Campanian Ignimbrite (39 ka) eruptions, and are lacking for lower-magnitude
829 events. To overcome this issue and to achieve a most comprehensive data set of
830 Mediterranean explosive volcanism, efforts should be made to date also tephras from
831 small-scale eruptions in sedimentary archives.
- 832 3. The similarity of major element glass composition of tephras from the same source
833 volcanoes (i.e., Campi Flegrei, Ischia) often prevents a reliable correlation with a
834 specific event. This problem can be overcome by additional trace element analyses
835 (e.g., Smith et al., 2011; Tomlinson et al., in press) and $^{87}\text{Sr}/^{86}\text{Sr}$ isotopic
836 measurements (e.g., Di Renzo et al., 2007; Giaccio et al., 2007; Roulleau et al., 2009).

837 Those data in addition to the comprehensive Monticchio tephra data set will contribute to an
838 improved Late Quaternary tephrostratigraphy in the Mediterranean.

839
840
841
842
843

844 **Acknowledgments**

845 We thank D. Berger, M. Köhler, M. Prena, R. Scheuss, and D. Axel for the retrieval of
846 sediment cores during the coring campaign in 2000. Special thanks are due to G. Arnold, M.
847 Köhler and D. Berger for thin section preparation, O. Appelt and V. Smith for technical
848 support during EPMA measurements and A. Hendrich and M. Dziggel for graphical support.
849 The coring campaign and tephra studies were funded by the GFZ German Research Centre for
850 Geosciences, Potsdam, Germany. This study is a contribution to the Helmholtz-Association
851 climate initiative REKLIM (Topic 8 ‘Rapid Climate Change from Proxy data’).

852

853

854 **References**

- 855 Albert, P.G., Tomlinson, E.L., Smith, V.C., Di Roberto, A., Todman, A., Rosi, M., Marani,
856 M., Müller, W., Menzies, M.A., 2012. Marine-continental tephra correlations: Volcanic glass
857 geochemistry from the Marsili Basin And the Aeolian Islands, Southern Tyrrhenian Sea, Italy.
858 *Journal of Volcanology and Geothermal Research* 229-230, 74-94.
- 859 Albore Livadie, C., D'Amore, L., 1980. Palma Campania (Napoli). Resti di abitato dell'età del
860 Bronzo Antico. *Notizie degli Scavi di Antichità* 34, 59-101.
- 861 Alessio, M., Bella, F., Improta, S., Belluomini, G., Calderoni, G., Cortesi, C., Turi, B., 1973.
862 University of Rome Carbon-14 dates X. *Radiocarbon* 15, 165 - 178.
- 863 Alessio, M., Bella, F., Improta, S., Belluomini, G., Calderoni, G., Cortesi, C., Turi, B., 1974.
864 University of Rome Carbon-14 dates XII. *Radiocarbon* 16, 358 - 367.
- 865 Alessio, M., Bella, F., Improta, S., Belluomini, G., Calderoni, G., Cortesi, C., Turi, B., 1976.
866 University of Rome Carbon-14 dates XIV. *Radiocarbon* 18, 321 - 349.
- 867 Alessio, M., Bella, F., Improta, S., Belluomini, G., Cortesi, C., Turi, B., 1971. University of
868 Rome Carbon-14 dates IX. *Radiocarbon* 13, 395 - 411.
- 869 Allen, J.R.M., Brandt, U., Brauer, A., Hubberten, H.-W., Huntley, B., Keller, J., Kraml, M.,
870 Mackensen, A., Mingram, J., Negendank, J.F.W., Nowaczyk, N.R., Oberhänsli, H., Watts,
871 W.A., Wulf, S., Zolitschka, B., 1999. Rapid environmental changes in southern Europe during
872 the last glacial period. *Nature* 400, 740-743.
- 873 Andronico, D., 1997. La Stratigrafia dei prodotti dell'eruzione di Lago Amendolare (Campi
874 Flegrei, Napoli). *Atti Società Toscana di Scienze naturali Memorie, Serie A* 104, 165-178.
- 875 Andronico, D., Calderoni, G., Cioni, R., Sbrana, A., Sulpizio, R., Santacroce, R., 1995.
876 Geological map of Somma-Vesuvius Volcano. *Periodico di Mineralogia* 64, 77 - 78.
- 877 Beccaluva, L., Gabbianelli, G., Lucchini, F., Rossi, P.L., Savelli, C., 1985. Petrology and
878 K/Ar ages of volcanics dredged from the Eolian seamounts: implications for geodynamic
879 evolution of the southern Tyrrhenian basin. *Earth and Planetary Science Letters* 74, 187-208.
- 880 Bertagnini, A., Landi, P., Rosi, M., Vigliargio, A., 1998. The Pomici di Base plinian eruption
881 of Somma-Vesuvius. *Journal of Volcanology and Geothermal Research* 83, 219 - 239.
- 882 Bourne, A.J., Lowe, J.J., Trincardi, F., Asioli, A., Blockley, S., Wulf, S., Matthews, I.P., Piva,
883 A., Vigliotti, L., 2010. Distal tephra record for the last ca 105,000 years from core PRAD 1-2

- 884 in the central Adriatic Sea: implications fro marine tephrostratigraphy. *Quaternary Science*
885 *Reviews* 29, 3079-3094.
- 886 Branca, S., Coltelli, M., De Beni, E., Wijbrans, J., 2008. Geological evolution of Mount Etna
887 volcano (Italy) from earliest products until the first central volcanism (between 500 and 100
888 ka ago) inferred from geochronological and stratigraphic data. *International Journal of Earth*
889 *Science* 97, 135-152.
- 890 Brandt, U., Nowaczyk, N.R., Ramrath, A., Brauer, A., Mingram, J., Wulf, S., Negendank,
891 J.F.W., 1999. Palaeomagnetism of Holocene and Late Pleistocene sediments from Lago di
892 Mezzano and Lago Grande di Monticchio (Italy): initial results. *Quaternary Science Reviews*
893 18, 961-976.
- 894 Brauer, A., Allen, J.R.M., Mingram, J., Dulski, P., Wulf, S., Huntley, B., 2007. Evidence for
895 last interglacial chronology and environmental change from Southern Europe. *Proceedings of*
896 *the National Academy of Sciences* 104, 450-455.
- 897 Brauer, A., Endres, C., Negendank, J.F.W., 1999. Lateglacial calendar year chronology based
898 on annually laminated sediments from Lake Meefelder Maar, Germany. *Quaternary*
899 *International* 61, 17-25.
- 900 Brauer, A., Mingram, J., Frank, U., Günter, C., Schettler, G., Wulf, S., Zolitschka, B.,
901 Negendank, J.F.W., 2000. Abrupt environmental oscillations during the Early Weichselian
902 recorded at Lago Grande di Monticchio, southern Italy. *Quaternary International* 73/74, 79-
903 90.
- 904 Brocchini, D., La Volpe, L., Laurenzi, M.A., Principe, C., 1994. Storia evolutiva del Monte
905 Vulture. *Plinius* 12, 22-25.
- 906 Buccheri, G., Bertoldo, G., Coppa, M.G., Munno, R., Pennetta, M., Siani, G., Valente, A.,
907 Secchione, C., 2002a. Studio multidisciplinare della successione sedimentaria tardo-
908 quaternaria proveniente dalla scarpata continentale del Golfo di Policastro (Tirreno
909 meridionale). *Bollettino della Societa Geologica Italiana* 121, 187-210.
- 910 Buccheri, G., Capretto, G., Di Donato, V., Esposito, p., Ferruzza, G., Pescatore, T., Russo
911 Ermolli, E., Senatore, M.R., Sprovieri, M., Bertoldo, G., Carella, D., Madonia, G., 2002b. A
912 high resolution record of the last deglaciation in the southern Tyrrhenian Sea: environmental
913 and climatic evolution. *Marine Geology* 186, 447-470.
- 914 Calanchi, N., Dinelli, E., 2008. Tephrostratigraphy of the last 170 ka in sedimentary
915 successions from the Adriatic Sea. *Journal of Volcanology and Geothermal Research* 177, 81-
916 95.
- 917 Capaldi, G., Civetta, L., Gillot, P.Y., 1985. Geochronology of Plio-Pleistocene volcanic rocks
918 from southern Italy. *Rendiconti della Societa Italiana di Mineralogia e Petrologia* 40, 25 - 44.
- 919 Coltelli, M., Del Carlo, P., Vezzoli, L., 2000. Stratigraphic constraints for explosive activity
920 in the past 100 ka at Etna Volcano, Italy. *International Journal of Earth Sciences* 89, 665-677.
- 921 de Vita, S., Orsi, G., Civetta, L., Carandente, A., D' Antonio, M., Deino, A., di Cesare, T., Di
922 Vito, M.A., Fisher, R.V., Isaia, R., Marotta, E., Necco, A., Ort, M., Pappalardo, L., Piochi,
923 M., Southon, J., 1999. The Agnano-Monte Spina eruption (4100 years BP) in the restless
924 Campi Flegrei caldera (Italy). *Journal of Volcanology and Geothermal Research* 91, 269-301.
- 925 De Vivo, B., Rolandi, G., Gans, P.B., Calvert, A., Bohrsen, W.A., Spera, F.J., Belkin, H.E.,
926 2001. New constraints on the pyroclastic eruptive history of the Campanian volcanic plain
927 (Italy). *Mineralogy and Petrology* 73, 47-65.

- 928 Deino, A.L., Curtis, G.H., Southon, J., Terrasi, F., Campajola, L., Orsi, G., 1994. ^{14}C and
929 $^{40}\text{Ar}/^{39}\text{Ar}$ dating of the Campanian Ignimbrite, Phlegrean Fields, Italy, *ICOG-8*, Berkeley, CA,
930 p. 77.
- 931 Deino, A.L., Orsi, G., de Vita, S., Piochi, M., 2004. The age of the Neapolitan Yellow Tuff
932 caldera-forming eruption (Campi Flegrei caldera - Italy) assessed by $^{40}\text{Ar}/^{39}\text{Ar}$ dating method.
933 *Journal of Volcanology and Geothermal Research* 133, 157-170.
- 934 Delibrias, G., Di Paola, G.M., Rosi, M., Santacroce, R., 1979. La storia eruttiva del complesso
935 vulcanico Somma Vesuvio ricostruita dalle successioni piroclastiche del Monte Somma.
936 *Reniconti Societa Italiana di Mineralogia e Petrologia* 35, 411 - 438.
- 937 Delibrias, G., Guillier, M.-T., Labeyrie, J., 1986. Gif natural radiocarbon measurements X.
938 *Radiocarbon* 28, 9 - 68.
- 939 Di Renzo, V., Di Vito, M.A., Arienzo, I., Carandente, A., Civetta, L., D'Antonio, M.,
940 Giordano, F., Orsi, G., Tonarini, S., 2007. Magmatic history of Somma-Vesuvius on the basis
941 of new geochemical and isotopic data from a deep borehole (Camaldoli della Torre). *Journal*
942 *of Petrology* 48, 753-784.
- 943 Di Vito, M., Isaia, R., Orsi, G., Southon, J., di Vita, S., D' Antonio, M., Pappalardo, L.,
944 Piochi, M., 1999. Volcanism and deformation since 12,000 years at the Campi Flegrei caldera
945 (Italy). *Journal of Volcanology and Geothermal Research* 91, 221-246.
- 946 Di Vito, M.A., Sulpizio, R., Zanchetta, G., D'Orazio, M., 2008. The late Pleistocene
947 pyroclastic deposits of the Campanian Plain: New insights into the explosive activity of
948 Neapolitan volcanoes. *Journal of Volcanology and Geothermal Research* 177, 19-48.
- 949 Esperança, S., Crisci, G.M., de Rosa, R., Mazzuoli, R., 1992. The role of the crust in the
950 magmatic evolution of the island of Lipari (Aeolian Islands, Italy). *Contributions to*
951 *Mineralogy and Petrology* 112, 450-462.
- 952 Fedele, F.G., Giaccio, B., Isaia, R., Orsi, G., 2002. Ecosystem impact of the Campanian
953 Ignimbrite eruption in Late Pleistocene Europe. *Quaternary Research* 57, 420-424.
- 954 Freda, C., Gaeta, M., Karner, D.B, Marra, F., Renne, P.R., Taddeucci, J., Scarlato, P.,
955 Christensen, J.N., Dallai, L., 2006. Eruptive history and petrologic evolution of the Albano
956 multiple maar (Alban Hills, Central Italy). *Bulletin of Volcanology* 68, 567-591.
- 957 Fuchs, C.W.C., 1873. Monografia geologica dell'isola d'Ischia, con carta geologica 1:25.000.
958 Mem. per serv. alla descrizione carta geologica d'Italia 2/1, 1.
- 959 Funk, S., 2004. Mikrofazielle Untersuchungen an Seesedimenten des Zeitfensters 37 - 25 ka
960 vor heute aus dem Lago Grande di Monticchio, Italien, und deren paläoklimatische
961 Bedeutung, Institute for Geosciences. University of Potsdam, Potsdam, p. 94.
- 962 Gertisser, R., Keller, J., 2000. From basalt to dacite: origin and evolution of the calc-alkaline
963 series of Salina, Aeolian Arc, Italy. *Contributions to Mineralogy and Petrology* 139, 607-626.
- 964 Giaccio, B., Isaia, R., Fedele, F.G., Di Canzio, E., Hoffecker, J., Ronchitelli, A., Sinitsyn,
965 A.A., Anikovich, M., Lisitsyn, S.N., Popov, V.V., 2008. The Campanian Ignimbrite and
966 Codola tephra layers: Two temporal/stratigraphic markers for the Early Upper Palaeolithic in
967 southern Italy and eastern Europe. *Journal of Volcanology and Geothermal Research* 177,
968 208-226.
- 969 Giaccio, B., Sposato, A., Gaeta, M., Marra, F., Palladino, D.M., Taddeucci, J., Barbieri, M.,
970 Messina, P., Rolfo, M.F., 2007. Mid-distal occurrences of the Albano Maar pyroclastic
971 deposits and their relevance for reassessing the eruptive scenarios of the most recent activity

- 972 at the Colli Albani Volcanic District, Central Italy. *Quaternary International* 171-172, 160-
973 178.
- 974 Giaccio, B., Marra, F., Hajdas, I., Karner, D.B., Renne, P.R., Sposato, A., 2009. $^{40}\text{Ar}/^{39}\text{Ar}$ and
975 ^{14}C geochronology of the Albano maar deposits: Implications for defining the age and
976 eruptive style of the most recent explosive activity at Colli Albani Volcanic District, Central
977 Italy. *Journal of Volcanology and Geothermal Research* 185, 203-213.
- 978 Giaccio, B., Nomade, S., Wulf, S., Isaia, R., Sottili, G., Cavuoto, G., Galli, P., Messina, P.,
979 Sposato, A., Sulpizio, R., Zanchetta, G., submitted. The late MIS 5 Mediterranean tephra
980 markers: a reappraisal from peninsular Italy terrestrial records. *Quaternary Science Reviews*.
- 981 Gillot, P.-Y., Keller, J., 1993. Radiochronological dating of Stromboli. *Acta Vulcanologica* 3,
982 69-77.
- 983 Gillot, P.Y., 1987. Histoire volcanique des îles éoliennes: arc insulaire ou complexe
984 orogénique annulaire?, IGAL Paris, pp. 35-42.
- 985 Gillot, P.Y., Chiesa, S., Pasquare, G., Vezzoli, L., 1982. <33.000 yr K/Ar dating of the
986 volcano-tectonic horst of the isle of Ischia, Gulf of Naples. *Nature* 299, 242-245.
- 987 Hornig-Kjarsgaard, I., Keller, J., Koberski, U., Stadlbauer, E., Francalanci, L., Lenhart, R.,
988 1993. Geology, stratigraphy and volcanological evolution of the island of Stromboli, Aeolian
989 arc, Italy. *Acta Vulcanologica* 3, 21-68.
- 990 Hunt, J.B., Hill, P.G., 1996. An inter-laboratory comparison of the electron probe
991 microanalysis of glass geochemistry. *Quaternary International* 34-36, 229-241.
- 992 Keller, J., 1980. The island of Salina. *Rendiconti Società Italiana di Mineralogia e Petrologia*
993 36, 489-524.
- 994 Keller, J., Ryan, W.B.F., Ninkovich, D., Altherr, R., 1978. Explosive volcanic activity in the
995 Mediterranean over the past 200,000 yr as recorded in deep-sea sediments. *Geological Society*
996 *of America Bulletin* 89, 591 - 604.
- 997 Keller, J., Kraml, M., 2004. Tephrochronological archives for known and unknown
998 paroxysms in Italian explosive volcanism of the upper Quaternary. IAVCEI General
999 Assembly Nov. 2004, Pucón, Chile.
- 1000 Kraml, M., 1997. Laser- $^{40}\text{Ar}/^{39}\text{Ar}$ -Datierungen an distalen marinen Tephren des jung-quartären
1001 mediterranen Vulkanismus (Ionisches Meer, METEOR-Fahrt 25/4), Geowissenschaftliche
1002 Fakultät. Albert-Ludwigs-Universität Freiburg i.Br., Freiburg i. Br., p. 216.
- 1003 Laurenzi, M.A., Villa, I.M., 1987. $^{40}\text{Ar}/^{39}\text{Ar}$ chronostratigraphy of Vico ignimbrites. *Periodico*
1004 *di Mineralogia* 56, 285-293.
- 1005 Le Bas, M.J., Le Maitre, R.W., Streckeisen, A., Zanettin, B., 1986. A chemical classification
1006 of volcanic rocks based on the Total Alkali-Silica diagram. *Journal of Petrology* 27, 745 -
1007 750.
- 1008 Lowe, J.J., Blockley, S., Trincardi, F., Asioli, A., Cattaneo, A., Matthews, I.P., Pollard, M.,
1009 Wulf, S., 2007. Age modelling of late Quaternary marine sequences in the Adriatic: Towards
1010 improved precision and accuracy using volcanic event stratigraphy. *Continental Shelf*
1011 *Research* 27, 560-582.

- 1012 Lucchi, F., Tranne, C.A., De Astis, G., Keller, J., Losito, R., Morche, W., 2008. Brown Tuffs
1013 on the Aeolian Islands (southern Italy). *Journal of Volcanology and Geothermal Research* 177
1014 (1), 49-70.
- 1015 Mahood, G.A., Hildreth, W., 1986. Geology of the peralkaline volcano at Pantelleria, Strait of
1016 Sicily. *Bulletin of Volcanology* 48, 143-172.
- 1017 Marciano, R., Munno, R., Petrosino, P., Santo, A.P., Villa, I., 2008. Late quaternary tephra
1018 layers along the Cilento coastline (southern Italy). *Journal of Volcanology and Geothermal*
1019 *Research* 177, 227-243.
- 1020 Marra, F., Deocampo, D., Jackson, M.D., Ventura, G., 2011. The Alban Hills and Monti
1021 Sabatini volcanic products used in ancient Roman masonry (Italy): An integrated stratigraphic,
1022 archaeological, environmental and geochemical approach. *Earth-Science Reviews* 108, 115-
1023 136.
- 1024 Marzocchella, A., Calderoni, G., Nisbet, R., 1994. Sarno e Frattaminore: evidenze dagli
1025 abitati, In: Livadie, A. (Ed.), *L'eruzione vesuviana delle "Pomici di Avellino" e la facies di*
1026 *Palma Campania (Bronzo Antico)*. Edipuglia, Bari, pp. 157-202.
- 1027 Morche, W., 1988. Tephrochronologie der Äolischen Inseln. *Mineralogisch-Petrologisches*
1028 *Institut, Universität Freiburg/Br.*, p. 238.
- 1029 Munno, R., Petrosini, P., 2007. The late Quaternary tephrostratigraphical record of the San
1030 Gregorio Magno basin (southern Italy). *Journal of Quaternary Science* 22, 247-266.
- 1031 Nappi, G., Mattioli, M., 2003. Evolution of the Sabatinian Volcanic District (central Italy) as
1032 inferred by stratigraphic successions of its northern sector and geochronological data.
1033 *Periodico di Mineralogia* 72, 79-102.
- 1034 Narcisi, B., 1996. Tephrochronology of a late quaternary lacustrine record from the
1035 Monticchio Maar (Vulture Volcano, southern Italy). *Quaternary Science Reviews* 15, 155 -
1036 165.
- 1037 Newton, A.J., Dugmore, A.J., 1993. Tephrochronology of Core C from Lago Grande di
1038 Monticchio, In: Negendank, J.F.W., Zolitschka, B. (Eds.), *Paleolimnology of European Maar*
1039 *Lakes*. Springer-Verlag, Berlin, Heidelberg, pp. 333 - 348.
- 1040 Nicotra, E., Ferlito, C., Viccaro, M., Cristofolini, R., 2011. Volcanic geology and petrology of
1041 the Val Calanna succession (Mt. Etna, Southern Italy): discovery of a new eruptive center.
1042 *Periodico di Mineralogia* 80, 287-307.
- 1043 Pantosti, D., Schwartz, D.P., Valenise, G., 1993. Paleoseismology along the 1980 surface
1044 rupture of the Irpinia Fault: implications for the Earthquake recurrence in the Southern
1045 Apennines, Italy. *Journal of Geophysical Research* 98, 6561-6577.
- 1046 Pappalardo, L., Civetta, L., D'Antonio, M., Deino, A., Di Vito, M., Orsi, G., Carandente, A.,
1047 de Vita, S., Isaia, R., Piochi, M., 1999. Chemical and Sr-isotopic evolution of the Phlegrean
1048 magmatic system before the Campanian Ignimbrite and the Neapolitan Yellow Tuff eruptions.
1049 *Journal of Volcanology and Geothermal Research* 91, 141-166.
- 1050 Passariello, I., Livadie, C.A., Talamo, P., Lubritto, C., D'Onofrio, A., Terrasi, F., 2009. ¹⁴C
1051 chronology of Avellino pumices eruption and timing of human reoccupation of the devastated
1052 region. *Radiocarbon* 51, 803-816.
- 1053 Paterne, M., 1985. Reconstruction de l'activité explosive des volcans de l'Italie du Sud par
1054 tephrochronologie marine. Thèse Doctorat-Etat, Université Paris-Sud Orsay, 141 pp.

- 1055 Paterne, M., Guichard, F., Duplessy, J.C., Siani, G., Sulpizio, R., Labeyrie, J., 2008. A
 1056 90,000-200,000 yrs marine tephra record of Italian volcanic activity in the Central
 1057 Mediterranean Sea. *Journal of Volcanology and Geothermal Research* 177, 187-196.
- 1058 Paterne, M., Guichard, F., Labeyrie, J., Gillot, P.Y., Duplessy, J.C., 1986. Tyrrhenian Sea
 1059 tephrochronology of the oxygen isotope record for the past 60,000 years. *Marine Geology* 72,
 1060 259 - 285.
- 1061 Paterne, M., Guichard, F., Labeyrie, J., 1988. Explosive activity of the South Italian volcanoes
 1062 during the past 80,000 yrs as determined by marine tephrochronology. *Journal of*
 1063 *Volcanology and Geothermal Research* 34, 153-172.
- 1064 Paterne, M., Labeyrie, J., Guichard, F., Mazaud, A., Maitre, F., 1990. Fluctuations of the
 1065 Campanian explosive volcanic activity (South Italy) during the past 190,000 years, as
 1066 determined by marine tephrochronology. *Earth and Planetary Science Letters* 98, 166 - 174.
- 1067 Perini, G., Conticelli, S., Francalanci, L., 1997. Inferences on the volcanic history of the Vico
 1068 volcano, Roman Magmatic Province, Central Italy: stratigraphic, petrographic and
 1069 geochemical data. *Mineralogica et Petrographica Acta* 40, 67-93.
- 1070 Perini, G., Francalanci, L., Davidson, J.P., Conticelli, S., 2004. Evolution and genesis of
 1071 magmas from Vico Volcano, central Italy: Multiple differentiation pathways and variable
 1072 parental magmas. *Journal of Petrology* 45, 139-182.
- 1073 Poli, S., Chiesa, S., Gillot, P.-Y., Guichard, F., Vezzoli, L., 1989. Time dimension in the
 1074 geochemical approach and hazard estimates of a volcanic area: the Isle of Ischia case (Italy).
 1075 *Journal of Volcanology and Geothermal Research* 36, 327 - 335.
- 1076 Radicati di Brozolo, F., Di Girolamo, P., Turi, B., Oddone, M., 1988. ^{40}Ar - ^{39}Ar and K-Ar
 1077 dating of K-rich rocks from the Roccamonfina Volcano, Roman Comagmatic Region, Italy.
 1078 *Geochimica et Cosmochimica Acta* 52, 1435 - 1441.
- 1079 Reimer, P.J., Baillie, M.G.L., Bard, E., Bayliss, A., Beck, J.W., Blackwell, P.G., Bronk
 1080 Ramsey, C., Buck, C.E., Burr, G.S., Edwards, R.L., Friedrich, M., Grootes, P.M., Guilderson,
 1081 T.P., Hajdas, I., Heaton, T.J., Hogg, A.G., Hughen, K.A., Kaiser, K.F., Kromer, B.,
 1082 McCormac, F.G., Manning, S.W., Reimer, R.W., Richards, D.A., Southon, J.R., Talamo, S.,
 1083 Turney, C.S.M., van der Plicht, J., Weyhenmeyer, C.E., 2009. IntCal09 and Marine09
 1084 radiocarbon age calibration curves, 0–50,000 years cal BP. *Radiocarbon* 51,1111–1150.
- 1085 Rittmann, A., 1930. *Geologie der Insel Ischia*, Zeitschrift für Vulkanologie ErgänzungsBand
 1086 6, Berlin.
- 1087 Rolandi, G., Barrella, A.M., Borrelli, A., 1993. The 1631 eruption of Vesuvius. *Journal of*
 1088 *Volcanology and Geothermal Research* 58, 183 - 201.
- 1089 Rolandi, G., Petrosino, P., McGeehin, J., 1998. The interplinian activity at Somma-Vesuvius
 1090 in the last 3500 years. *Journal of Volcanology and Geothermal Research* 82, 19 - 52.
- 1091 Romano, R., 1982. Succession of the volcanic activity in the Etnean area. *Memorie della*
 1092 *Società Geologica Italiana* 23, 27-48.
- 1093 Rosi, M., Sbrana, A., 1987. *Phlegrean Fields*. CNR, Roma.
- 1094 Roulleau, E., Pinti, D.L., Rouchon, V., Quidelleur, X., Gillot, P.-Y. 2009. Tephro-
 1095 chronostratigraphy of the lacustrine interglacial record of Piànico, Italian Southern Alps:
 1096 Identifying the volcanic sources using radiogenic isotopes and trace elements. *Quaternary*
 1097 *International* 204, 31-43.

- 1098 Santacroce, R., Cioni, R., Marianelli, P., Sbrana, A., Sulpizio, R., Zanchetta, G., Donahue,
1099 D.J., Joron, J.L., 2008. Age and whole rock-glass compositions of proximal pyroclastics from
1100 the major explosive eruptions of Somma-Vesuvius: A review as a tool for distal
1101 tephrostratigraphy. *Journal of Volcanology and Geothermal Research* 177, 1-18.
- 1102 Scandone, R., Bellucci, F., Lirer, L., Rolandi, G., 1991. The structure of the Campanian Plain
1103 and the activity of the Neapolitan volcanoes (Italy). *Journal of Volcanology and Geothermal*
1104 *Research* 48, 1 - 31.
- 1105 Scheld, A., 1995. Tephralagen in "METEOR-Kernen" des Ionischen Meeres. Universität
1106 Freiburg i.Br., p. 83.
- 1107 Sevink, J., van Bergen, M.J., van der Plicht, J., Feiken, H., Anastasia, C., Huizinga, A., 2011.
1108 Robust date for the Bronze Age Avellino eruption (Somma-Vesuvius): 3945 +/- 10 calBP
1109 (1995 +/- 10 calBC). *Quaternary Science Reviews* 30, 1035-1046.
- 1110 Siani, G., Paterne, M., Michel, E., Sulpizio, R., Sbrana, A., Arnold, M., Haddad, G., 2001.
1111 Mediterranean Sea surface radiocarbon reservoir age changes since the last glacial maximum.
1112 *Science* 294, 1917-1920.
- 1113 Siani, G., Sulpizio, R., Paterne, M., Sbrana, A., 2004. Tephrostratigraphy study for the last
1114 18,000 ¹⁴C years in a deep-sea sediment sequence for the South Adriatic. *Quaternary Science*
1115 *Reviews* 23, 2485-2500.
- 1116 Sinitsyn, A.A., 2003. A Palaeolithic "Pompeii" at Kostenki, Russia. *Antiquity* 77, 9-14.
- 1117 Smith, V.C., Isaia, R., Pearce, N.J.G., 2011. Tephrostratigraphy and glass compositions of
1118 post-15 kyr Campi Flegrei eruptions: implications for eruption history and chronostratigraphic
1119 markers. *Quaternary Science Reviews* 30, 3638-3660.
- 1120 Sollevanti, F., 1983. Geologic, volcanologic, and tectonic setting of the Vico-Cimino area,
1121 Italy. *Journal of Volcanology and Geothermal Research* 17, 203-217.
- 1122 Sottili, G., Palladino, D.M., Gaeta, M., Masotta, M., 2012. Origins and energetics of maar
1123 volcanoes: examples from the ultrapotassic Sabatini Volcanic District (Roman Province,
1124 Central Italy). *Bulletin of Volcanology* 74, 163-186.
- 1125 Sottili, G., Palladino, D.M., Marra, F., Jicha, B., Karner, D.B., Renne, P., 2010.
1126 Geochronology of the most recent activity in the Sabatini Volcanic District, Roman Province,
1127 central Italy. *Journal of Volcanology and Geothermal Research* 196, 20-30.
- 1128 Stoppa, F., Principe, C., 1998. Eruption style and petrology of a new carbonatitic suite from
1129 the Mt. Vulture (Southern Italy): The Monticchio Lakes Formation. *Journal of Volcanology*
1130 *and Geothermal Research* 80, 137-153.
- 1131 Stuiver, M., Reimer, P.J., 1993. Extended ¹⁴C data base and revised calib 3.0 ¹⁴C age
1132 calibration program. *Radiocarbon* 35, 215 - 230.
- 1133 Sulpizio, R., Zanchetta, G., D'Orazio, M.D., Vogel, H., Wagner, B., 2010. Tephrostratigraphy
1134 and tephrochronology of lakes Ohrid and Prespa, Balkans. *Biogeosciences Discussions* 7,
1135 3931-3967.
- 1136 Sulpizio, R., Zanchetta, G., Paterne, M., Siani, G., 2003. A review of tephrostratigraphy in
1137 central and southern Italy during the last 65 ka. *Il Quaternario* 16, 91-108.
- 1138 Terrasi, L., Campajola, F., Petrazuolo, V., Roca, M., Romano, A., Brondi, A., D'Onofrio, M.,
1139 Romoli, R., Monito, K., 1994. Datazione con la spettrometria di massa ultrasensibile di
1140 campioni provenienti dall'area interessata dall'eruzione delle "Pomici di Avellino", In:

- 1141 Livadie, A. (Ed.), L'eruzione vesuviana delle "Pomici di Avellino" e la facies di Palma
1142 Campania (Bronzo Antico). Edipuglia, Bari, pp. 139-146.
- 1143 Tomlinson, E.L., Arienzo, I., Civetta, L., Wulf, S., Smith, V.C., Hardiman, M., Lane, C.S.,
1144 Carandente, A., Orsi, G., Rosi, M., Müller, W., Thirlwall, M.F., Menzies, M.A., in press.
1145 Geochemistry of the Phlegrean Fields (Italy) proximal sources for major Mediterranean
1146 tephras. *Geochimica et Cosmochimica Acta*.
- 1147 Ton-That, T., Singer, B., Paterne, M., 2001. $^{40}\text{Ar}/^{39}\text{Ar}$ dating of latest Pleistocene (41 ka)
1148 marine tephra in the Mediterranean Sea: implications for global climate records. *Earth and*
1149 *Planetary Science Letters* 184, 645-658.
- 1150 Trua, T., Serri, G., Marani, M., Renzulli, A., Gamberi, F., 2002. Volcanological and
1151 petrological evolution of Marsili Seamount (southern Tyrrhenian Sea). *Journal of*
1152 *Volcanology and Geothermal Research* 114, 441-464.
- 1153 Vezzoli, L., 1988. *Island of Ischia*. CNR, Roma.
- 1154 Vezzoli, L., 1991. Tephra layers in Bannock Basin (Eastern Mediterranean). *Marine Geology*
1155 100, 21 - 34.
- 1156 Villa, I.M., Buettner, A., 2009. Chronostratigraphy of Monte Vulture volcano (southern Italy):
1157 secondary mineral microtextures and ^{39}Ar - ^{40}Ar systematic. *Bulletin of Volcanology* 71,
1158 1195-1208.
- 1159 Vogel, J.S., Cornell, W., Nelson, D.E., Southon, J.R., 1990. Vesuvius/Avellino, one possible
1160 source of seventeenth century BC climatic disturbances. *Nature* 344, 534 - 537.
- 1161 Watts, W.A., 1985. A long pollen record from Laghi di Monticchio, southern Italy: a
1162 preliminary account. *Journal of the Geological Society, London*, 142, 491-499.
- 1163 Watts, W.A., Allen, J.R.M., Huntley, B., Fritz, S.C., 1996a. Vegetation history and climate of
1164 the last 15,000 years at Laghi di Monticchio, southern Italy. *Quaternary Science Reviews* 15,
1165 113-132.
- 1166 Wulf, S., Brauer, A., Kraml, M., Keller, J., Negendank, J.F.W., 2004. Tephrochronology of
1167 the 100 ka lacustrine sediment record of Lago Grande di Monticchio (southern Italy).
1168 *Quaternary International* 122, 7-30.
- 1169 Wulf, S., Brauer, A., Mingram, J., Zolitschka, B., Negendank, J.F.W., 2006. Distal tephras in
1170 the sediments of Monticchio maar lakes, In: Principe, C. (Ed.), *La geologia del monte*
1171 *Vulture*. Consiglio Nazionale delle Ricerche, pp. 105-122.
- 1172 Wulf, S., Kraml, M., Keller, J., 2008. Towards a detailed distal tephrostratigraphy in the
1173 Central Mediterranean: The last 20,000 yrs record of Lago Grande di Monticchio. *Journal of*
1174 *Volcanology and Geothermal Research* 2008, 118-132.
- 1175 Zanchetta, G., Sulpizio, R., Roberts, N., Cioni, R., Eastwood, W.J., Siani, G., Caron, B.,
1176 Paterne, M., Santacroce, R., 2011. Tephrostratigraphy, chronology and climatic events of the
1177 Mediterranean basin during the Holocene: An overview. *The Holocene* 21, 33-52.
- 1178 Zolitschka, B., Negendank, J.F.W., 1996. Sedimentology, dating and palaeoclimatic
1179 interpretation of a 76.3 ka record from Lago Grande di Monticchio, southern Italy. *Quaternary*
1180 *Science Reviews* 15, 101 - 112.
- 1181
- 1182
- 1183

1184 **Table captions**

1185

1186 **Table 1:** Core depths, composite depths, varve ages, thicknesses, maximum grain sizes and
1187 sources of Monticchio tephra layers deposited between 100 and 133 ka BP. CP=Campanian
1188 Province, E=Etna, PF=Phlegrean Fields, STR=Stromboli Island, IS=Ischia Island,
1189 SAL=Salina Island, SAB=Sabatini Volcanic District.

1190

1191 **Table 2:** Mean values of non-normalized EPMA glass data and 2σ standard deviation (*italics*)
1192 of tephra layers occurring in the Monticchio sequence between 100 and 133 ka BP. Totals are
1193 corrected for chlorine concentrations. Full analytical data of individual glass measurements
1194 are provided in Supplementary Table A.

1195

1196 **Table 3:** List of major element data of distal and proximal tephras used for correlation with
1197 Monticchio tephras (see text). Data from: * this study; (1) Paterne et al. (2008), (2) Sulpizio et
1198 al. (2010), (3) Di Vito et al., (2008), (4) Sottili et al. (2012), (5) Poli et al. (1987), (6) Fuchs
1199 (1873).

1200

1201 **Table 4:** Revised tephrochronology of Lago Grande di Monticchio for the last 133 kyrs. V =
1202 Vesuvius; PF = Campi Flegrei; E = Etna; PV = Procida-Vivara; A = Alban Hills; IS = Ischia;
1203 STR = Stromboli; PA = Pantelleria; CP = Campanian Volcanic Province; RP = Roman
1204 Province. Conventional and AMS radiocarbon dating were calibrated using CALIB 6.0.1 with
1205 the IntCal09 or Marine09 calibration curves (Stuiver and Reimer, 1993; Reimer et al., 2009).
1206 Age references for correlatives: (1) Rolandi et al. (1993), (2) Rolandi et al. (1998), (3) Vogel
1207 et al. (1990), (4) Terrasi et al. (1994), (5) Santacroce et al. (2008), (6) Andronico et al. (1995),
1208 (7) Watts et al. (1996a), (8) Pantosti et al. (1993), (9) Zanchetta et al. (2011), (10) Passariello
1209 et al. (2009), (11) Sevink et al. (2011), (12) Alessio et al. (1973), (13) Albore Livadie and
1210 D'Amore (1980), (14) Delibrias et al. (1986), (15) Marzocchella et al. (1994), (16) Rosi and
1211 Sbrana (1987), (17) de Vita et al. (1999), (18) Alessio et al. (1971), (19) Siani et al. (2004),
1212 (20) Alessio et al. (1974), (21) Di Vito et al. (1999), (22) Deino et al. (2004), (23) Pappalardo
1213 et al. (1999), (24) Andronico (1997), (25) Branca et al. (2008), (26) Kraml (1997), (27) Siani
1214 et al. (2001), (28) Delibrias et al. (1979), (29) Capaldi et al. (1985), (30) Bertagnini et al.
1215 (1998), (31) Alessio et al. (1976), (32) Sulpizio et al. (2003), (33) Buccheri et al. (2002a), (34)
1216 Buccheri et al. (2002b), (35) Giaccio et al. (2008), (36) Giaccio et al. (2009), Freda et al.
1217 (2006), (37) De Vivo et al. (2001), (38) Deino et al. (1994), (39) Ton-That et al. (2001), (40)

1218 Fedele et al. (2002), (41) Sinitsyn (2003), (42) Gillot et al. (1982), (43) Gillot and Keller
1219 (1993), (44) Paterne et al. (1990), (45) Giaccio et al. (submitted), (46) Keller and Kraml
1220 (2004).

1221

1222

1223 **Figure captions**

1224 **Figure 1:** a) Site map of Italy showing major volcanic centres, the location of Lago Grande di
1225 Monticchio and distal correlation sites mentioned in the text. b) Bathymetric map of Lago
1226 Grande di Monticchio with coring sites.

1227

1228 **Figure 2:** Lithology and tephrostratigraphy of the composite profile LGM-B/D/E/J/M/O with
1229 focus on the 100-133 ka BP tephras.

1230

1231 **Figure 3:** Images under optical microscope of prominent tephras in the 100–133 ka BP
1232 sediment section of Lago Grande di Monticchio. **a)** TM-25; **b)** TM-30-1c; **c)** TM-26.

1233

1234 **Figure 4a:** Harker diagram SiO₂ vs. CaO for chemical discrimination of Monticchio tephras
1235 from the Campanian Province (undefined): ⁽¹⁾ mean SEM-EDS glass data (Munno and
1236 Petrosino, 2007; Marciano et al., 2008); ⁽²⁾ SEM-EDS glass data (Paterne et al., 2008); ⁽³⁾
1237 EPMA glass data (Scheld, 1995); ⁽⁴⁾ EPMA glass data (Wulf et al., 2004; this study); ⁽⁵⁾
1238 EPMA glass data (Giaccio et al., submitted); ⁽⁶⁾ SEM-EDS glass data (Sulpizio et al., 2010).

1239

1240 **Figure 4b:** Harker diagram SiO₂ vs. FeO for chemical discrimination of Monticchio tephras
1241 from Mount Etna: ⁽¹⁾ XRF whole rock data of pyroclasts (Nicotra et al., 2011); ⁽²⁾ SEM-EDS
1242 glass data (this study); ⁽³⁾ XRF whole rock data of pyroclasts (Coltelli et al., 2000); ⁽⁴⁾ EPMA
1243 glass data (Wulf et al., 2004; Wulf et al., 2008); ⁽⁵⁾ XRF whole rock data of lava (M. Viccaro,
1244 this study).

1245

1246 **Figure 4c:** Harker diagram SiO₂ vs. CaO for chemical discrimination of Monticchio tephras
1247 TM-29, TM-30 and TM-31 from the Campanian volcanic province (Phlegrean Fields?): ⁽¹⁾
1248 SEM-EDS glass data (Di Vito et al., 2008); ⁽²⁾ SEM-EDS glass data (Sulpizio et al., 2010).

1249

1250 **Figure 4d:** Harker diagram SiO₂ vs. alkali ratio for chemical discrimination of Monticchio
1251 tephras from Stromboli Island: ⁽¹⁾ EPMA glass data (Wulf et al., 2004); ⁽²⁾ XRF whole rock

1252 data (Hornig-Kjarsgaard et al., 1993); ⁽³⁾ XRF whole rock data (Trua et al., 2002); ⁽⁴⁾ XRF
1253 whole rock data (Beccaluva et al., 1985); ⁽⁵⁾ EPMA glass data (this study, see Supplementary
1254 Table C).

1255

1256 **Figure 4e:** Harker diagram SiO₂ vs. CaO for chemical discrimination of Monticchio tephras
1257 from Ischia Island: ⁽¹⁾ XRF whole rock data (Poli et al., 1987); ⁽²⁾ wet whole rock data
1258 (Rittmann, 1930); ⁽³⁾ wet whole rock data (Fuchs, 1873); ⁽⁴⁾ SEM-EDS glass data (Paterne et
1259 al., 2008); ⁽⁵⁾ SEM-EDS glass data (Paterne, 1985; this study).

1260

1261 **Figure 4f:** Harker diagram SiO₂ vs. CaO for chemical discrimination of Monticchio tephras
1262 from Salina Island: ⁽¹⁾ XRF whole rock (Gertisser and Keller, 2000); ⁽²⁾ XRF whole rock
1263 (Esperança et al., 1992); ⁽³⁾ EPMA glass data (Albert et al., 2012; this study, see
1264 Supplementary Table C); ⁽⁴⁾ EPMA glass data, this study (see Supplementary Table C).

1265

1266 **Figure 4g:** Harker diagram SiO₂ vs. TiO₂ for chemical discrimination of Monticchio tephras
1267 from the Sabatini Volcanic District: ⁽¹⁾ XRF whole rock data (Perini et al., 1997; (Perini et al.,
1268 2004); ⁽²⁾ EPMA glass data (Sottili et al., 2012).

1269

1270 **Figure 5:** Synthesis of revised tephrochronology and varve-supported sedimentation rate
1271 chronology of the 133 ka Monticchio sequence (upper diagram) and 2σ age uncertainties
1272 calculated by the discrepancy between mean radiometric/radioisotopic and Monticchio varve
1273 ages of tephras (lower diagram).

Table 1

Tephra layer	Core depth (base of tephra)	Composite depth (m)	Varve age (cal. yrs BP) $\pm 2\sigma$ error	Thickness (mm)	Maximum grain size (μm)	Source
TM-25	M49u, 97.5 cm	74.11	105,480 \pm 1050	113.0	1500	CP
TM-26	O49u, 40.4 cm	74.47	106,300 \pm 1060	1.0	80	E
TM-27	O53u, 45.6 cm	78.85	108,330 \pm 1080	2000.0	1300	CP
TM-28	a M59u, 48.8 cm	81.44	110,410 \pm 1100	21.0	160	CP
	b M59u, 52.5 cm	81.53	110,830 \pm 1110	2.0	400	CP
TM-29-1	a M59u, 68.5 cm	81.69	111,480 \pm 1110	0.6	280	PF ?
	b O58u, 16.4 cm	81.86	112,180 \pm 1120	1.0	100	PF ?
	c O58u, 16.7 cm	81.87	112,210 \pm 1120	1.0	180	PF ?
	d O58u, 16.8 cm	81.87	112,230 \pm 1120	0.2	100	PF ?
	e O58u, 17.0 cm	81.87	112,230 \pm 1120	0.5	190	PF ?
	f O58u, 17.3 cm	81.87	112,250 \pm 1120	2.3	300	PF ?
	g O58u, 17.9 cm	81.88	112,310 \pm 1120	0.3	100	PF ?
	h O58u, 18.6 cm	81.88	112,330 \pm 1120	5.0	400	PF ?
	i O58u, 21.7 cm	81.91	112,460 \pm 1120	4.0	260	PF ?
TM-29-2	a M62u, 60.5 cm	82.06	112,520 \pm 1130	6.0	220	PF ?
	b M62u, 60.9 cm	82.07	112,540 \pm 1130	2.5	160	PF ?
	c M62u, 61.1 cm	82.08	112,560 \pm 1130	0.5	110	PF ?
	d M62u, 61.5 cm	82.08	112,580 \pm 1130	2.5	200	PF ?
	e M62u, 63.0 cm	82.10	112,620 \pm 1130	4.0	140	PF ?
	f M62u, 67.3 cm	82.13	112,790 \pm 1130	7.0	180	PF ?
	g M62u, 73.4 cm	82.20	112,990 \pm 1130	16.0	400	PF ?
	h M62u, 73.9 cm	82.20	113,020 \pm 1130	2.5	140	PF ?
TM-30-1	a M62u, 79.5 cm	82.26	113,370 \pm 1140	2.0	100	PF ?
	b M62u, 80.9 cm	82.28	113,490 \pm 1140	3.0	280	PF ?
	c M64u, 20.7 cm	82.55	113,660 \pm 1140	18.0	300	PF ?
	d M64u, 20.8 cm	82.55	113,670 \pm 1140	0.5	100	PF ?
	e M64u, 26.9 cm	82.61	113,880 \pm 1140	1.0	90	PF ?
	f M64u, 33.9 cm	82.67	114,000 \pm 1140	12.0	700	PF ?
TM-30-2	a M64u, 39.3 cm	82.74	114,440 \pm 1140	1.5	300	PF ?
	b M64u, 40.5 cm	82.75	114,530 \pm 1150	2.0	300	PF ?
	c M64u, 42.0 cm	82.76	114,600 \pm 1150	8.0	100	PF ?
	d M64u, 43.9 cm	82.78	114,720 \pm 1150	12.0	800	PF ?
TM-31	M64u, 44.5 cm	82.79	114,770 \pm 1150	0.5	180	PF ?
TM-32	M64u, 50.2 cm	82.85	115,250 \pm 1150	1.0	120	STR ?
TM-33-1	a M64u, 71.2 cm	83.05	115,720 \pm 1160	10.0	320	IS
	b M64u, 71.5 cm	83.06	115,750 \pm 1160	1.0	100	IS
	c M64u, 75.5 cm	83.10	116,110 \pm 1160	4.0	240	IS
TM-33-2	a M65u, 28.0 cm	83.43	118,190 \pm 1180	0.3	110	IS
	b M65u, 28.7 cm	83.43	118,210 \pm 1180	4.0	250	IS
TM-34	M65u, 39.8 cm	83.54	118,810 \pm 1190	0.4	100	SAL ?
TM-35	a O62u, 63.0 cm	84.14	120,670 \pm 1210	3.0	650	CP
	b O63u, 59.5 cm	84.84	121,940 \pm 1220	3.5	230	CP
TM-36	M70u, 22.9 cm	85.30	123,030 \pm 1230	1.5	300	SAB
TM-37	a M70u, 61.5 cm	85.68	124,080 \pm 1240	11.0	200	IS
	b M71o, 76.3 cm	86.18	124,330 \pm 1240	8.0	500	IS
	c M71o, 80.3 cm	86.22	124,360 \pm 1240	1.5	150	IS
	d M71u, 13.0 cm	86.59	124,860 \pm 1250	1.0	90	IS
TM-38	M72o, 64.0 cm	87.07	125,550 \pm 1260	0.4	150	CP
TM-39	O70u, 52.7 cm	91.98	130,530 \pm 1310	6.0	170	CP
TM-40	O70u, 88.0 cm	92.37	130,860 \pm 13,090	5.0	170	CP (IS?)
TM-41	M77u, 34.0 cm	92.77	131,020 \pm 13,100	6.0	300	CP (IS?)
TM-42	O74u, 70.3 cm	97.69	132,110 \pm 13,210	1.0	300	IS

Table 2

Sample	TM-25	TM-26	TM-27	TM-28a	TM-28b	TM-29-1a
SiO ₂	59.10 <i>1.37</i>	64.23 <i>1.57</i>	60.11 <i>0.76</i>	60.22 <i>0.65</i>	60.75 <i>0.74</i>	49.39 <i>0.53</i>
TiO ₂	0.39 <i>0.05</i>	0.54 <i>0.09</i>	0.45 <i>0.03</i>	0.46 <i>0.03</i>	0.48 <i>0.02</i>	1.14 <i>0.04</i>
Al ₂ O ₃	17.95 <i>0.39</i>	16.82 <i>1.25</i>	18.17 <i>0.26</i>	18.41 <i>0.18</i>	18.45 <i>0.19</i>	17.81 <i>0.21</i>
FeO	3.32 <i>0.34</i>	3.38 <i>0.59</i>	2.79 <i>0.15</i>	2.94 <i>0.21</i>	3.09 <i>0.08</i>	8.57 <i>0.31</i>
MnO	0.13 <i>0.02</i>	0.13 <i>0.03</i>	0.23 <i>0.06</i>	0.25 <i>0.05</i>	0.29 <i>0.03</i>	0.15 <i>0.03</i>
MgO	0.62 <i>0.13</i>	0.94 <i>0.37</i>	0.40 <i>0.08</i>	0.28 <i>0.03</i>	0.31 <i>0.02</i>	3.52 <i>0.15</i>
CaO	2.54 <i>0.30</i>	3.14 <i>0.75</i>	1.80 <i>0.10</i>	1.74 <i>0.12</i>	1.71 <i>0.11</i>	8.71 <i>0.25</i>
Na ₂ O	3.85 <i>0.23</i>	4.78 <i>0.34</i>	6.19 <i>0.70</i>	5.97 <i>0.52</i>	6.11 <i>0.41</i>	2.69 <i>0.16</i>
K ₂ O	8.31 <i>0.18</i>	3.79 <i>0.48</i>	7.10 <i>0.48</i>	6.30 <i>0.17</i>	6.61 <i>0.14</i>	5.58 <i>0.30</i>
P ₂ O ₅	0.16 <i>0.05</i>	0.21 <i>0.04</i>	0.06 <i>0.04</i>	0.04 <i>0.02</i>	0.04 <i>0.02</i>	0.94 <i>0.06</i>
Cl	0.39 <i>0.03</i>	0.25 <i>0.04</i>	0.70 <i>0.14</i>	0.83 <i>0.14</i>	0.89 <i>0.04</i>	0.25 <i>0.02</i>
Total	96.67	98.14	97.86	97.25	98.63	98.70
Analyses	n=10	n=9	n=22	n=10	n=16	n=13

Sample	TM-29-1b	TM-29-1c	TM-29-1d	TM-29-1e	TM-29-1f	TM-29-1g
SiO ₂	49.25 <i>1.14</i>	50.21 <i>0.32</i>	50.38 <i>0.58</i>	51.67 <i>1.65</i>	50.80 <i>0.32</i>	51.69 <i>0.60</i>
TiO ₂	1.10 <i>0.03</i>	1.12 <i>0.04</i>	1.10 <i>0.03</i>	1.11 <i>0.02</i>	1.10 <i>0.04</i>	1.09 <i>0.07</i>
Al ₂ O ₃	17.67 <i>0.45</i>	18.00 <i>0.11</i>	18.17 <i>0.06</i>	17.89 <i>0.37</i>	17.96 <i>0.20</i>	17.96 <i>0.12</i>
FeO	7.90 <i>0.17</i>	8.04 <i>0.12</i>	7.85 <i>0.13</i>	7.88 <i>0.15</i>	7.91 <i>0.18</i>	7.75 <i>0.23</i>
MnO	0.14 <i>0.02</i>	0.15 <i>0.01</i>	0.15 <i>0.03</i>	0.16 <i>0.03</i>	0.13 <i>0.02</i>	0.15 <i>0.03</i>
MgO	3.29 <i>0.15</i>	3.47 <i>0.15</i>	3.49 <i>0.29</i>	3.10 <i>0.40</i>	3.33 <i>0.22</i>	2.90 <i>0.36</i>
CaO	8.13 <i>0.21</i>	8.41 <i>0.32</i>	8.44 <i>0.60</i>	7.61 <i>0.98</i>	7.83 <i>0.37</i>	7.17 <i>0.63</i>
Na ₂ O	2.93 <i>0.04</i>	2.91 <i>0.06</i>	2.96 <i>0.12</i>	2.95 <i>0.11</i>	2.88 <i>0.06</i>	3.00 <i>0.16</i>
K ₂ O	5.78 <i>0.14</i>	5.80 <i>0.14</i>	5.75 <i>0.36</i>	5.79 <i>0.08</i>	5.87 <i>0.28</i>	6.36 <i>0.28</i>
P ₂ O ₅	0.77 <i>0.10</i>	0.70 <i>0.05</i>	0.73 <i>0.05</i>	0.68 <i>0.03</i>	0.69 <i>0.04</i>	0.72 <i>0.04</i>
Cl	0.35 <i>0.03</i>	0.34 <i>0.01</i>	0.34 <i>0.02</i>	0.33 <i>0.02</i>	0.35 <i>0.02</i>	0.40 <i>0.03</i>
Total	97.24	99.07	99.29	99.09	98.76	99.09
Analyses	n=5	n=7	n=5	n=5	n=8	n=5

Sample	TM-29-1h	TM-29-1i	TM-29-2a	TM-29-2b	TM-29-2c	TM-29-2d
SiO ₂	52.17 <i>1.27</i>	51.54 <i>1.03</i>	52.15 <i>1.24</i>	52.55 <i>0.79</i>	53.91 <i>0.52</i>	54.19 <i>0.34</i>
TiO ₂	1.02 <i>0.05</i>	1.10 <i>0.06</i>	1.06 <i>0.05</i>	1.09 <i>0.04</i>	1.13 <i>0.03</i>	1.09 <i>0.03</i>
Al ₂ O ₃	18.08 <i>0.32</i>	17.91 <i>0.23</i>	17.46 <i>0.33</i>	17.76 <i>0.35</i>	17.36 <i>0.17</i>	17.39 <i>0.17</i>
FeO	7.49 <i>0.36</i>	7.43 <i>0.22</i>	7.59 <i>0.26</i>	7.69 <i>0.27</i>	7.72 <i>0.06</i>	7.69 <i>0.22</i>
MnO	0.15 <i>0.03</i>	0.12 <i>0.02</i>	0.15 <i>0.03</i>	0.14 <i>0.02</i>	0.14 <i>0.03</i>	0.15 <i>0.04</i>
MgO	2.65 <i>0.57</i>	3.38 <i>0.36</i>	2.87 <i>0.39</i>	2.96 <i>0.38</i>	2.51 <i>0.16</i>	2.37 <i>0.11</i>
CaO	6.98 <i>0.86</i>	7.89 <i>0.72</i>	7.11 <i>0.94</i>	7.38 <i>0.63</i>	6.38 <i>0.32</i>	6.10 <i>0.21</i>
Na ₂ O	3.16 <i>0.35</i>	2.76 <i>0.12</i>	2.93 <i>0.21</i>	2.94 <i>0.21</i>	3.13 <i>0.09</i>	3.14 <i>0.04</i>
K ₂ O	6.01 <i>0.54</i>	5.56 <i>0.34</i>	5.54 <i>0.24</i>	5.56 <i>0.22</i>	5.85 <i>0.26</i>	5.90 <i>0.17</i>
P ₂ O ₅	0.67 <i>0.07</i>	0.66 <i>0.05</i>	0.65 <i>0.09</i>	0.69 <i>0.06</i>	0.67 <i>0.04</i>	0.64 <i>0.04</i>
Cl	0.37 <i>0.05</i>	0.33 <i>0.03</i>	0.32 <i>0.02</i>	0.32 <i>0.02</i>	0.33 <i>0.01</i>	0.33 <i>0.02</i>
Total	98.67	98.60	97.76	99.02	99.05	98.91
Analyses	n=15	n=16	n=9	n=14	n=5	n=14

Sample	TM-29-2e	TM-29-2f	TM-29-2g	TM-30-1a	TM-30-1b	TM-30-1c
SiO ₂	53.15 <i>1.19</i>	54.57 <i>0.91</i>	56.91 <i>2.04</i>	53.22 <i>0.72</i>	56.43 <i>0.70</i>	55.52 <i>0.70</i>
TiO ₂	1.04 <i>0.09</i>	1.13 <i>0.11</i>	0.82 <i>0.18</i>	0.75 <i>0.08</i>	0.60 <i>0.09</i>	0.80 <i>0.13</i>
Al ₂ O ₃	17.46 <i>0.45</i>	17.85 <i>0.21</i>	18.31 <i>1.06</i>	16.73 <i>0.77</i>	18.64 <i>1.30</i>	17.59 <i>0.46</i>
FeO	7.65 <i>0.35</i>	6.78 <i>0.32</i>	5.50 <i>1.26</i>	6.20 <i>0.42</i>	5.29 <i>0.58</i>	6.66 <i>0.83</i>
MnO	0.15 <i>0.03</i>	0.14 <i>0.03</i>	0.14 <i>0.03</i>	0.14 <i>0.03</i>	0.14 <i>0.04</i>	0.14 <i>0.04</i>
MgO	2.45 <i>0.24</i>	2.59 <i>0.32</i>	1.79 <i>0.83</i>	1.97 <i>0.21</i>	1.61 <i>0.29</i>	2.04 <i>0.49</i>
CaO	6.30 <i>0.64</i>	6.14 <i>0.53</i>	4.91 <i>1.25</i>	5.69 <i>0.57</i>	5.14 <i>0.88</i>	5.49 <i>0.86</i>
Na ₂ O	3.15 <i>0.20</i>	3.31 <i>0.17</i>	3.69 <i>0.25</i>	2.96 <i>0.18</i>	3.49 <i>0.16</i>	3.16 <i>0.17</i>
K ₂ O	5.89 <i>0.43</i>	6.07 <i>0.24</i>	6.35 <i>0.92</i>	5.77 <i>0.24</i>	6.26 <i>0.66</i>	6.35 <i>0.75</i>
P ₂ O ₅	0.65 <i>0.06</i>	0.64 <i>0.07</i>	0.38 <i>0.14</i>	0.51 <i>0.07</i>	0.37 <i>0.05</i>	0.47 <i>0.12</i>
Cl	0.33 <i>0.03</i>	0.33 <i>0.03</i>	0.37 <i>0.10</i>	0.32 <i>0.03</i>	0.28 <i>0.04</i>	0.40 <i>0.10</i>
Total	98.14	99.46	99.09	94.18	98.19	98.52
Analyses	n=15	n=19	n=18	n=6	n=10	n=12

Table 2 (continued)

Sample	TM-30-1d		TM-30-1e		TM-30-1f		TM-30-2b		TM-30-2c		TM-30-2d	
SiO ₂	54.64	0.91	55.76	0.78	57.95	1.89	52.39	0.90	54.24	0.73	59.85	0.80
TiO ₂	0.65	0.02	0.66	0.07	0.64	0.22	1.05	0.12	0.81	0.05	0.50	0.03
Al ₂ O ₃	17.70	0.68	17.62	0.61	17.54	0.33	17.71	0.64	18.02	0.25	17.91	0.44
FeO	5.93	0.19	5.55	1.15	5.00	1.38	7.17	0.69	6.68	0.35	3.76	0.29
MnO	0.16	0.03	0.14	0.04	0.12	0.03	0.15	0.03	0.15	0.02	0.16	0.03
MgO	1.56	0.08	1.32	0.35	1.30	0.71	2.85	0.44	2.65	0.25	0.88	0.15
CaO	5.01	0.51	4.46	0.78	4.21	1.20	6.60	0.74	6.29	0.34	3.20	0.34
Na ₂ O	3.41	0.30	3.49	0.25	3.48	0.33	3.12	0.49	3.04	0.11	4.14	0.30
K ₂ O	6.55	0.37	6.61	0.29	6.91	0.82	5.73	0.48	6.13	0.17	6.62	0.38
P ₂ O ₅	0.42	0.04	0.45	0.06	0.31	0.20	0.52	0.08	0.58	0.07	0.17	0.03
Cl	0.43	0.05	0.42	0.15	0.43	0.08	0.32	0.05	0.34	0.02	0.47	0.03
Total	96.37		96.37		97.80		97.60		98.90		97.57	
Analyses	n=5		n=6		n=13		n=10		n=11		n=10	

Sample	TM-31		TM-32		TM-33-1a		TM-33-1c		TM-33-2a		TM-33-2b	
SiO ₂	61.10	5.48	59.73	0.59	59.83	0.64	61.64	0.59	61.14	1.21	58.57	0.50
TiO ₂	0.73	0.18	0.77	0.04	0.46	0.02	0.67	0.03	0.62	0.01	0.43	0.02
Al ₂ O ₃	18.43	0.46	16.95	0.33	18.66	0.17	18.45	0.23	18.01	0.38	18.31	0.17
FeO	4.18	1.77	6.47	0.40	3.03	0.06	2.98	0.26	2.77	0.08	2.95	0.13
MnO	0.24	0.09	0.16	0.03	0.25	0.03	0.29	0.05	0.28	0.03	0.19	0.03
MgO	1.12	1.11	1.94	0.19	0.41	0.01	0.35	0.05	0.31	0.04	0.38	0.04
CaO	2.86	2.58	4.38	0.29	1.86	0.13	1.05	0.07	1.00	0.06	1.92	0.04
Na ₂ O	2.03	0.48	4.17	0.13	5.49	0.42	6.96	0.31	6.99	0.42	5.27	0.12
K ₂ O	5.58	0.64	4.76	0.24	7.27	0.07	5.75	0.14	5.74	0.18	7.40	0.10
P ₂ O ₅	0.22	0.25	0.45	0.05	0.06	0.02	0.05	0.03	0.06	0.03	0.07	0.02
Cl	0.59	0.16	0.37	0.04	0.77	0.03	0.69	0.04	0.70	0.02	0.65	0.03
Total	96.99		100.07		97.93		98.71		97.46		95.99	
Analyses	n=9		n=10		n=9		n=10		n=9		n=7	

Sample	TM-34		TM-35a		TM-36		TM-37a		TM-37b		TM-37c	
SiO ₂	56.13	1.53	58.99	0.58	54.00	0.83	60.68	0.60	60.87	0.83	60.84	0.67
TiO ₂	1.26	0.10	0.41	0.02	0.40	0.02	0.61	0.03	0.63	0.03	0.61	0.03
Al ₂ O ₃	15.69	0.74	18.66	0.21	19.56	0.26	17.91	0.18	17.89	0.41	18.10	0.32
FeO	9.46	0.83	2.86	0.09	3.53	0.41	2.61	0.11	2.56	0.03	2.62	0.14
MnO	0.21	0.03	0.17	0.04	0.17	0.01	0.23	0.04	0.22	0.03	0.25	0.06
MgO	2.88	0.37	0.40	0.02	0.27	0.04	0.31	0.01	0.33	0.01	0.35	0.05
CaO	6.85	0.61	2.18	0.05	4.55	0.33	1.07	0.03	1.10	0.02	1.11	0.07
Na ₂ O	3.81	0.26	5.14	0.16	5.29	0.36	6.63	0.35	6.44	0.42	7.12	0.58
K ₂ O	2.41	0.19	7.94	0.17	7.33	0.76	5.90	0.10	5.87	0.15	5.99	0.14
P ₂ O ₅	0.48	0.06	0.05	0.02	0.04	0.02	0.04	0.02	0.07	0.02	0.07	0.02
Cl	0.21	0.03	0.58	0.03	0.13	0.01	0.62	0.03	0.56	0.04	0.47	0.07
Total	99.35		97.26		95.24		96.46		96.41		97.44	
Analyses	n=15		n=7		n=10		n=8		n=7		n=7	

Sample	TM-37d		TM-38		TM-39		TM-40		TM-41		TM-42	
SiO ₂	61.10	0.45	57.58	0.60	56.67	0.51	60.37	0.84	59.07	1.26	61.89	0.53
TiO ₂	0.63	0.02	0.48	0.02	0.58	0.02	0.61	0.05	0.48	0.06	0.66	0.04
Al ₂ O ₃	18.17	0.16	19.03	0.12	18.35	0.23	18.09	0.16	19.17	0.56	18.65	0.19
FeO	2.55	0.11	3.34	0.08	4.39	0.25	2.78	0.22	2.60	0.75	2.53	0.09
MnO	0.19	0.03	0.17	0.03	0.19	0.02	0.19	0.04	0.12	0.04	0.20	0.03
MgO	0.36	0.02	0.68	0.02	0.93	0.07	0.49	0.13	0.58	0.18	0.40	0.02
CaO	1.16	0.06	2.48	0.05	3.21	0.09	1.61	0.31	2.33	0.45	1.28	0.06
Na ₂ O	6.47	0.28	4.49	0.26	4.79	0.25	5.67	0.31	4.34	0.70	5.84	0.56
K ₂ O	6.16	0.15	8.42	0.12	7.45	0.32	6.27	0.25	7.51	0.38	6.36	0.18
P ₂ O ₅	0.07	0.04	0.10	0.04	0.20	0.03	0.13	0.04	0.11	0.02	0.05	0.03
Cl	0.51	0.04	0.51	0.03	0.47	0.03	0.40	0.07	0.39	0.13	0.51	0.02
Total	97.25		97.28		97.13		96.50		96.61		98.25	
Analyses	n=13		n=13		n=11		n=9		n=11		n=19	

Table 3

<i>Distal tephra correlatives</i>												
Sample	<i>C-27</i>	<i>C-27</i>	<i>C-31</i>	<i>TAU1-b?</i>	<i>Sabatini rew?</i>	<i>C-34 reworked?</i>	<i>C-34</i>	<i>C-35</i>	<i>C-36</i>	<i>C-36</i>	<i>Etnean</i>	<i>Etnean</i>
	<i>KET 80-04</i>	<i>KET 80-04</i>	<i>KET 80-04</i>	<i>DED 87-08</i>	<i>DED 87-08</i>	<i>DED 87-08</i>	<i>DED 87-08</i>	<i>KET 82-22</i>	<i>KET 80-04</i>	<i>KET 80-04</i>	<i>KET 80-04</i>	<i>KET 80-04</i>
	<i>930-945 cm</i>	<i>930-945 cm</i>	<i>975-985 cm</i>	<i>1254 cm</i>	<i>1254 cm</i>	<i>1254 cm</i>	<i>1260 cm</i>	<i>485 cm</i>	<i>1083 cm</i>	<i>1083 cm</i>	<i>1095 cm</i>	<i>1141 cm</i>
SiO ₂	60.46	61.87	61.80	51.10	56.11 (0.37)	61.20 (0.60)	60.92 (0.78)	61.97	61.42	61.22	62.38	62.55
TiO ₂	0.47	0.40	0.45	1.70	0.76 (0.05)	0.46 (0.12)	0.42 (0.10)	0.44	0.30	0.44	0.85	0.83
Al ₂ O ₃	18.31	18.21	18.11	17.38	19.73 (0.08)	18.37 (0.19)	18.43 (0.25)	18.57	19.27	18.43	17.95	17.24
FeO	3.51	3.08	3.16	8.59	4.25 (0.20)	3.11 (0.28)	3.11 (0.15)	3.17	2.95	3.10	5.11	5.28
MnO	0.16	0.22	0.28	0.22	0.18 (0.05)	0.24 (0.12)	0.23 (0.10)	0.00	0.00	0.00	-	-
MgO	0.75	0.39	0.31	3.15	1.16 (0.10)	0.38 (0.21)	0.33 (0.12)	0.31	0.34	0.33	1.40	1.25
CaO	2.59	1.79	1.76	7.85	3.95 (0.09)	1.83 (0.47)	1.80 (0.19)	1.92	2.71	1.82	4.64	4.19
Na ₂ O	3.69	5.82	5.64	3.30	5.38 (0.35)	5.61 (1.29)	5.91 (0.38)	6.58	4.47	5.63	4.38	4.92
K ₂ O	9.23	7.10	7.34	5.38	7.67 (0.27)	7.81 (1.09)	7.63 (0.49)	7.05	8.55	7.63	3.30	3.22
P ₂ O ₅	0.01	0.00	0.02	0.77	0.15 (0.15)	0.00 (0.00)	0.01 (0.04)	0.00	0.00	0.00	-	-
Total	99.18	98.88	98.87	99.92	99.32	99.01	98.80	100.01	100.01	98.81	100.01	99.48
Age	<i>103.6 ka</i>	<i>103.6 ka</i>	<i>107 ka</i>	<i>115.2 ka</i>	<i>115.2 ka</i>	<i>115.2 ka</i>	<i>116.1 ka</i>	<i>121.5 ka</i>	<i>123.2 ka</i>	<i>125.4 ka</i>	<i>124.6 ka</i>	<i>130.2 ka</i>
Ref.	(1)	(1)	(1)	* N=1	* N=2	* N=18	* N=19	(1)	(1)	(1)	* N=1	* N=1

<i>Proximal tephra correlatives</i>													
Sample	<i>C-38</i>	<i>C-39</i>	<i>C-39</i>	<i>Lake Ohrid</i>	<i>Lake Ohrid</i>			<i>VDPI</i>	<i>Punta</i>	<i>Monte Vezzi</i>	<i>Upper</i>	<i>Lower</i>	
	<i>DED 87-08</i>	<i>DED 87-08</i>	<i>DED 87-08</i>	<i>Lake Ohrid</i>	<i>Lake Ohrid</i>	<i>TAU1-b sc</i>	<i>TAU1-b ch</i>	<i>Valle dei Preti</i>	<i>Imperatore</i>	<i>lavas</i>	<i>Scarrupata</i>	<i>Scarrupata</i>	
	<i>1370 cm</i>	<i>1370 cm</i>	<i>1370 cm</i>	<i>OT0701-7a</i>	<i>OT0701-7b</i>			<i>Sabatini</i>	<i>Ischia</i>	<i>Ischia</i>	<i>Ischia</i>	<i>Ischia</i>	
SiO ₂	61.22	62.61	61.95	50.86	58.30	51.99	62.13	54.28	63.56	61.05	62.85	61.74	62.63
TiO ₂	0.45	0.64	0.38	1.15	0.63	1.25	0.60	0.32	0.77	0.00	0.67	0.66	0.44
Al ₂ O ₃	18.44	18.12	18.26	18.55	19.75	19.33	18.56	19.76	19.09	18.35	18.76	17.91	18.84
Fe ₂ O ₃	-	-	-	-	-	-	-	-	1.99	4.21	2.17	2.78	0.89
FeO	3.08	2.75	3.05	8.33	3.62	7.10	2.98	2.78	1.37	2.12	0.81	0.25	1.63
MnO	0.21	0.22	0.12	0.22	0.15	0.23	0.17	0.25	0.24	0.04	0.18	0.21	0.09
MgO	0.22	0.15	0.49	3.19	0.82	2.76	0.68	0.15	0.81	0.90	0.42	0.29	0.51
CaO	1.65	1.01	2.06	8.47	3.41	7.10	2.48	3.05	1.00	2.05	0.86	0.65	1.37
Na ₂ O	5.90	6.85	4.18	3.27	4.54	4.00	4.59	6.41	5.54	5.94	6.57	6.37	4.27
K ₂ O	7.65	6.56	8.75	5.40	8.36	6.22	7.81	7.32	5.85	5.28	5.96	6.07	6.95
P ₂ O ₅	0.00	0.00	0.00	0.28	0.01	-	-	0.01	0.00	0.00	0.03	0.01	0.04
Total	98.82	98.91	99.24	99.99	99.99	99.98	100.00	94.36	101.37	100.26	99.27	96.92	97.67
Age	<i>137 ka</i>	<i>137 ka</i>	<i>137 ka</i>					<i>< 154 ka</i>	<i>118.5 ka</i>	<i>118.5 ka</i>	<i>126 ka</i>	<i>130 ka</i>	<i>≥133 ka</i>
Ref.	(1)	(1)	(1)	(2)	(2)	(3)	(3)	(4)	(5)	(6)	(5)	(5)	(5)

Table 4

Table 4

Monticchio Tephra	Tephra event (Source)	Monticchio varve age (calendar yrs BP)	Weighted mean age of tephra correlative (cal yr BP)	2 σ error range of ages of correlatives (cal yr BP)	Tephra dating method and (total number of dating) of correlatives	Reference (dating of correlative)
TM-1	AD 1631 (V)	90	319	319	Historical record	1
TM-2a	AD 512 (V)	1420	1,438	1438	Historical record	2
TM-2b	Pollena AD472 (V)	1440	1,478	1478	Historical record	2
TM-3b	AP3 (V)	4020	2,850	2,750 – 2,950	^{14}C (1)	2
TM-3c	AP2 (V)	4150	3,470	3,270 – 4,090	^{14}C (4)	2, 3, 4, 5
TM-4	Pomici di Avellino (V)	4310	3,950	3,480 – 4,780	^{14}C (27)	2, 3, 5, 6, 7, 8, 9, 10, 11, 12, 13, 14, 15
TM-5a	Agnano Mt. Spina (PF)	4620	4,740	4,090 – 5,590	^{14}C (9)	12, 16, 17, 18, 19
TM-6b	Pomici di Mercato (V)	9680	8,900	8,480 – 9,680	^{14}C (5)	5, 6, 14, 20
TM-7b	Pomici Principali (PF)	12,180	11,970	11,240 – 12,390	^{14}C (2)	19, 21
TM-8	NYT (PF)	14,120	13,570	12,580 – 15,650	$^{40}\text{Ar}/^{39}\text{Ar}$ (1), ^{14}C (14)	12, 16, 18, 19, 22
TM-9	VM1/GM1 (PF)	14,560	14,350	13,350 – 15,750	$^{40}\text{Ar}/^{39}\text{Ar}$ (1), ^{14}C (2)	19, 23
TM-10d	Lagno Amendolare (PF)	15,550	15,300	14,130 – 16,460	^{14}C (3)	7, 19, 24
TM-11	Biancavilla / Y-1 (E)	16,440	17,350	16,810 – 17,910	^{14}C (3)	14, 19, 26
TM-12	Pomici Verdoline (V)	17,560	18,920	17,070 – 20,330	^{14}C (7)	5, 6, 19, 27, 28
TM-13	Pomici di Base (V)	19,280	21,700	19,600 – 24,470	^{14}C (6), K/Ar (1)	5, 6, 19, 28, 29, 30
TM-14	Solchiaro (PV)	21,260	23,260	22,540 – 23,980	^{14}C (1)	31
TM-15	Y-3 (PF?)	27,260	30,600	30,180 – 31,130	^{14}C (3)	32, 33, 34
TM-16b	Codola (V/PF?)	31,120	34,270	32,530 – 36,010	^{14}C (1)	35
TM-17bc	Albano Unit 7 (A)	31,830	35,800	29,000 – 40,000	$^{40}\text{Ar}/^{39}\text{Ar}$ (3)	36
TM-18	CI / Y-5 (PF)	36,770	39,070	33,950 – 43,150	$^{40}\text{Ar}/^{39}\text{Ar}$ (5), ^{14}C (3)	7, 32, 37, 38, 39, 40, 41
TM-19	TVE _{ss} (IS)	60,060	55,110	46,250 – 67,950	$^{40}\text{Ar}/^{39}\text{Ar}$ (3), K/Ar (5)	7, 26, 42
TM-20	UMSA (IS)	61,370	56,000	48,000 – 64,000	$^{40}\text{Ar}/^{39}\text{Ar}$ (1)	26
TM-21	Petrazza / Y-9 (STR)	78,340	75,300	69,300 – 81,300	K/Ar (1)	43
TM-22	Ignimbrite Z / P-10 (PA)	89,130	84,000	80,000 – 88,000	Sapropel (1)	44
TM-23-11	POP1 / C-22 (CP or RP)	95,180	92,400	87,800 – 97,000	$^{40}\text{Ar}/^{39}\text{Ar}$ (2)	45
TM-25	X-5 / C-27 (CP)	105,480	106,090	101,000 – 109,000	$^{40}\text{Ar}/^{39}\text{Ar}$ (2)	26, 45
TM-27	X-6 / C-31 (CP)	108,330	109,000	105,000 – 113,000	Sapropel (1)	26, 46
TM-33-2b	Punta Imperatore / C-35 (IS)	118,210	118,460	110,750 – 128,350	K/Ar (4)	42

Figure 1

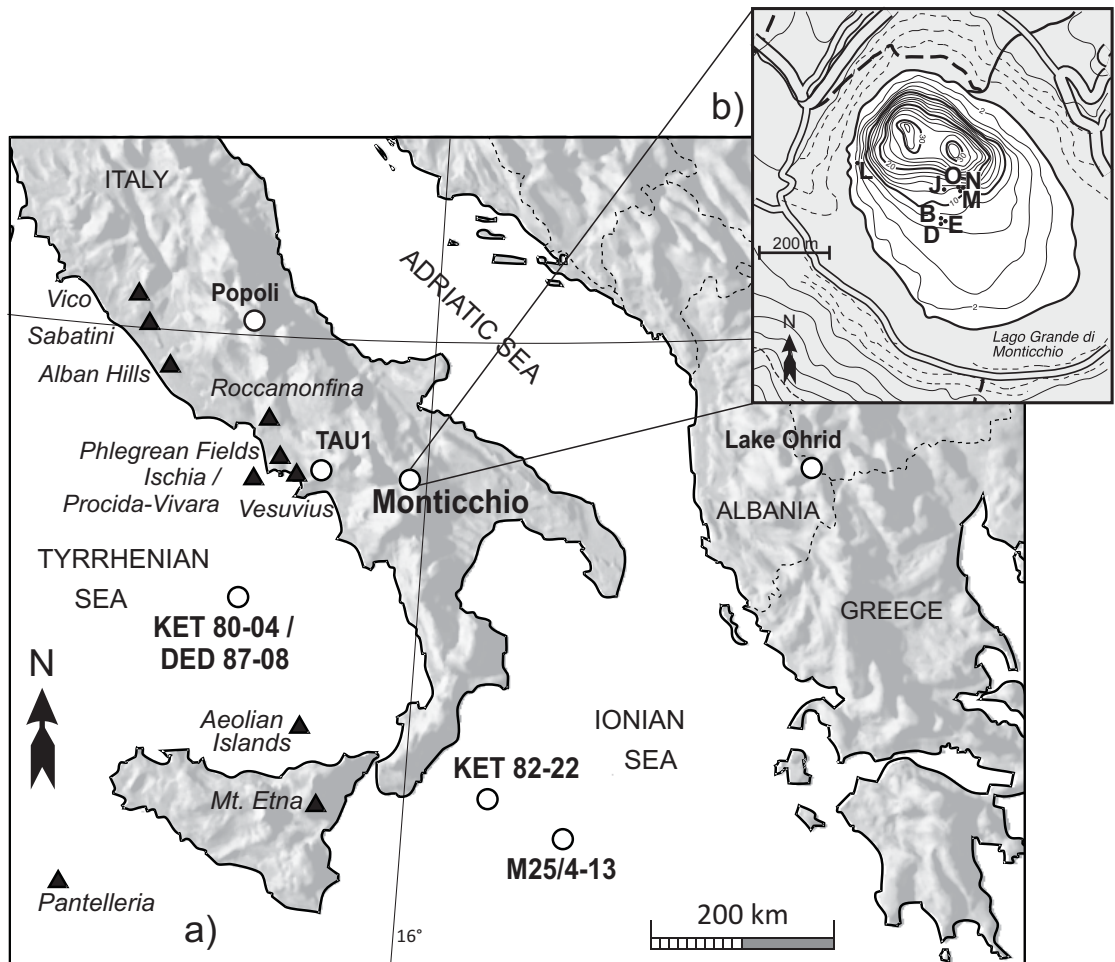


Figure 1

Figure 2

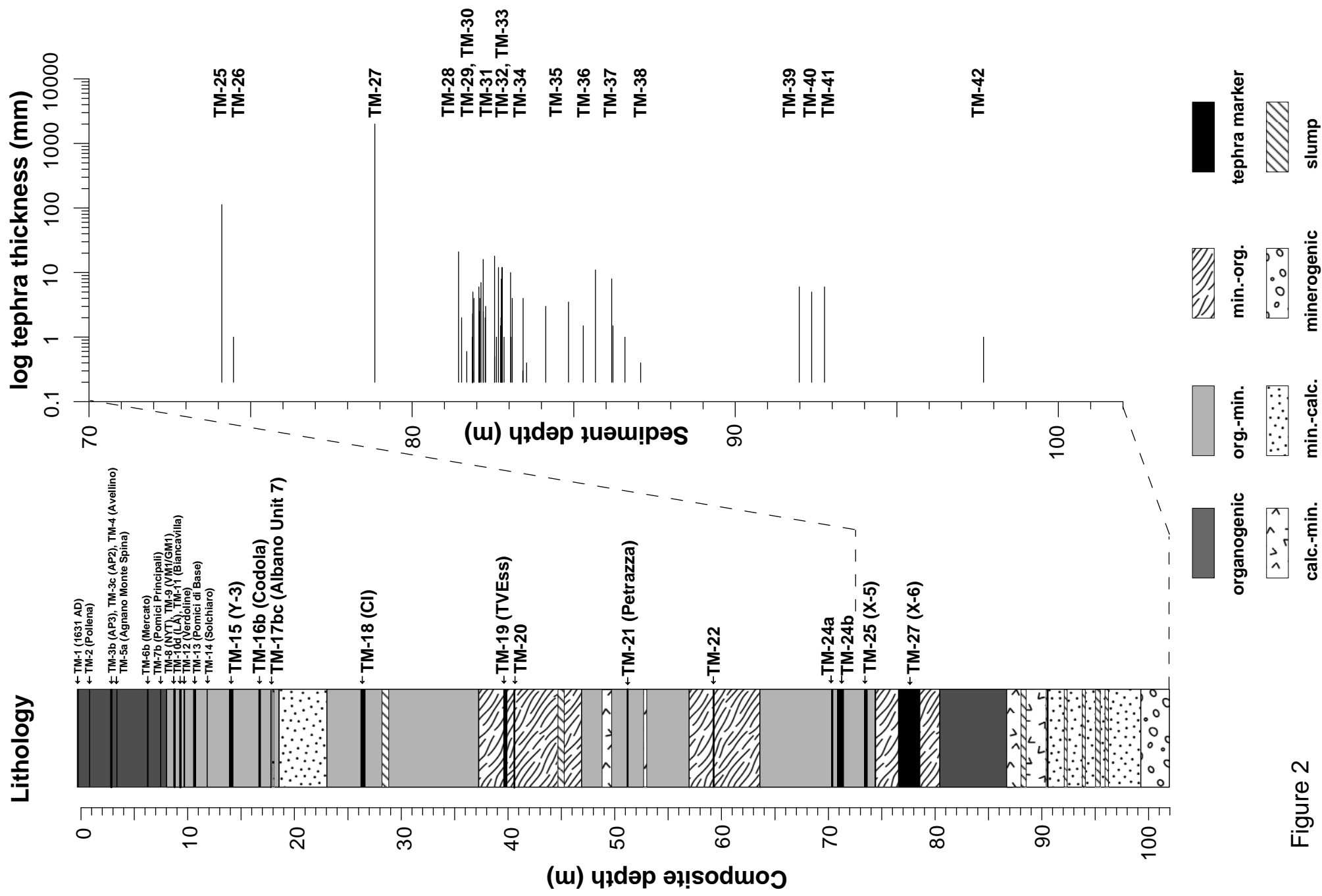


Figure 2

Figure 3

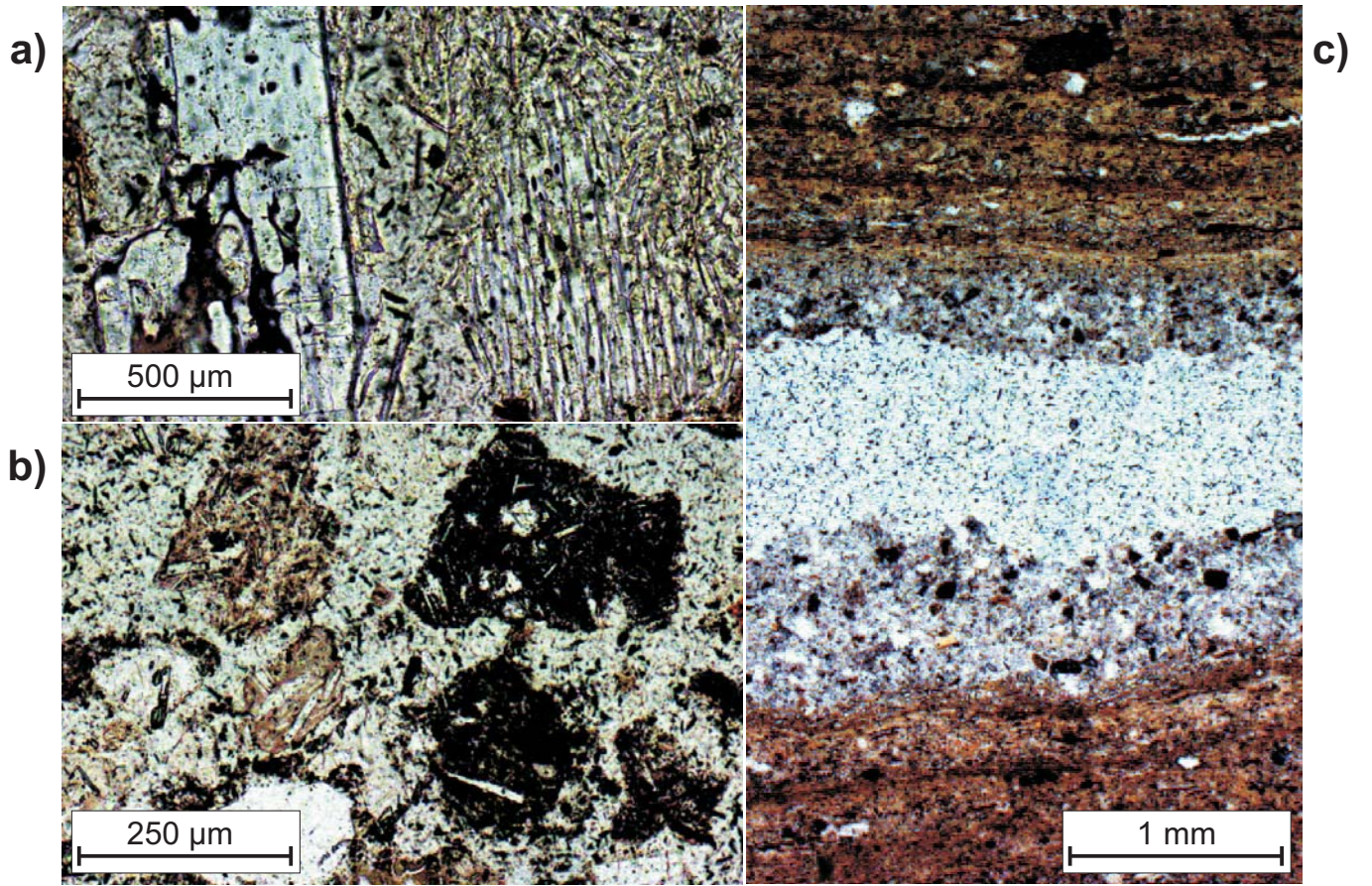


Figure 3

Figure 4a

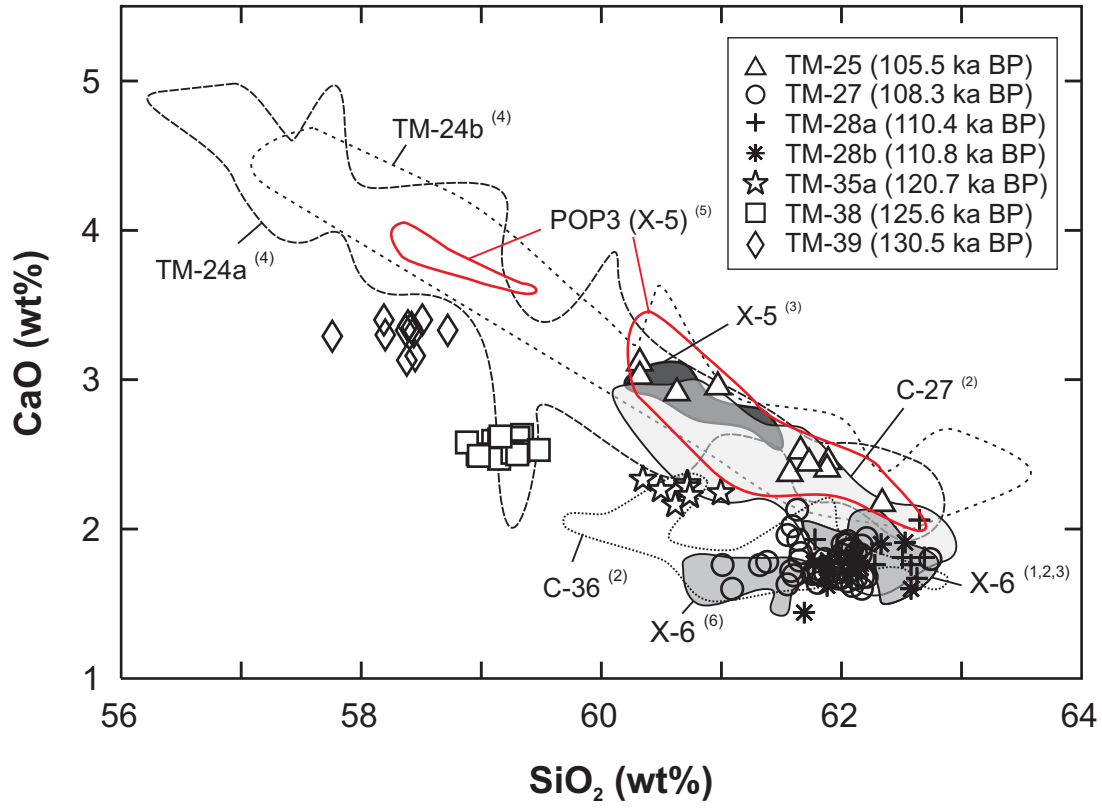


Figure 4a

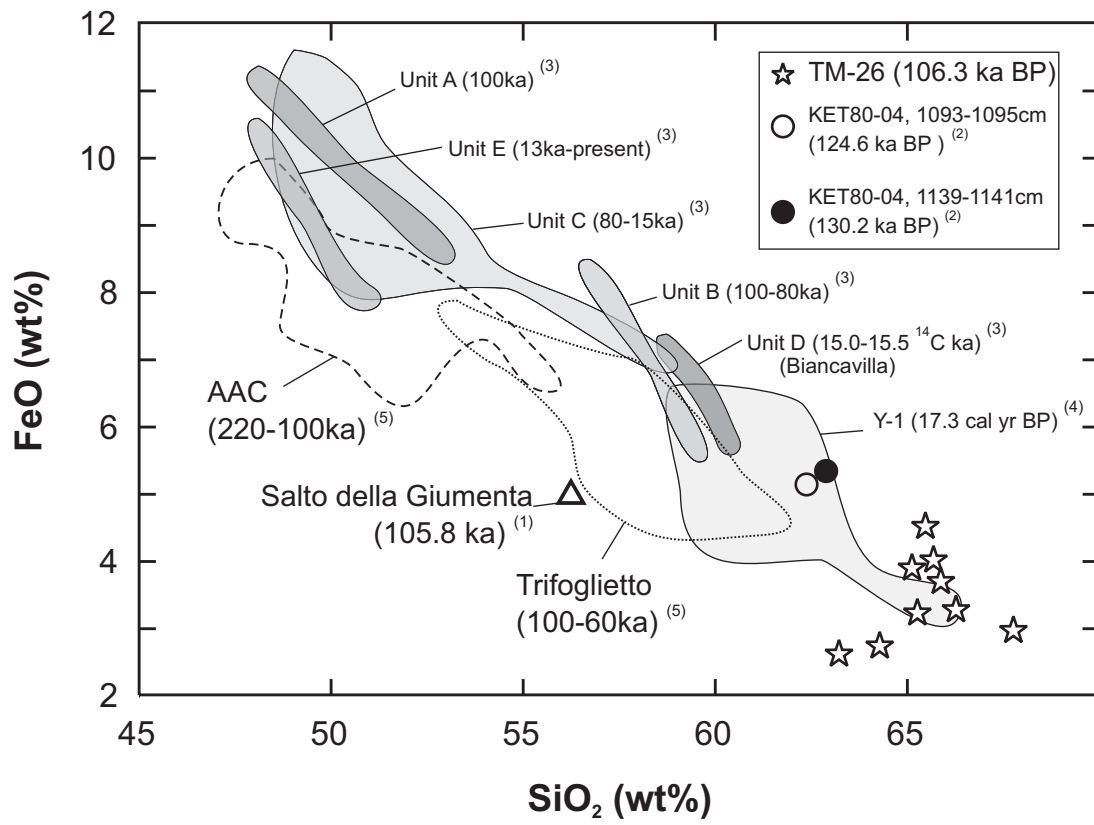


Figure 4b

Figure 4c

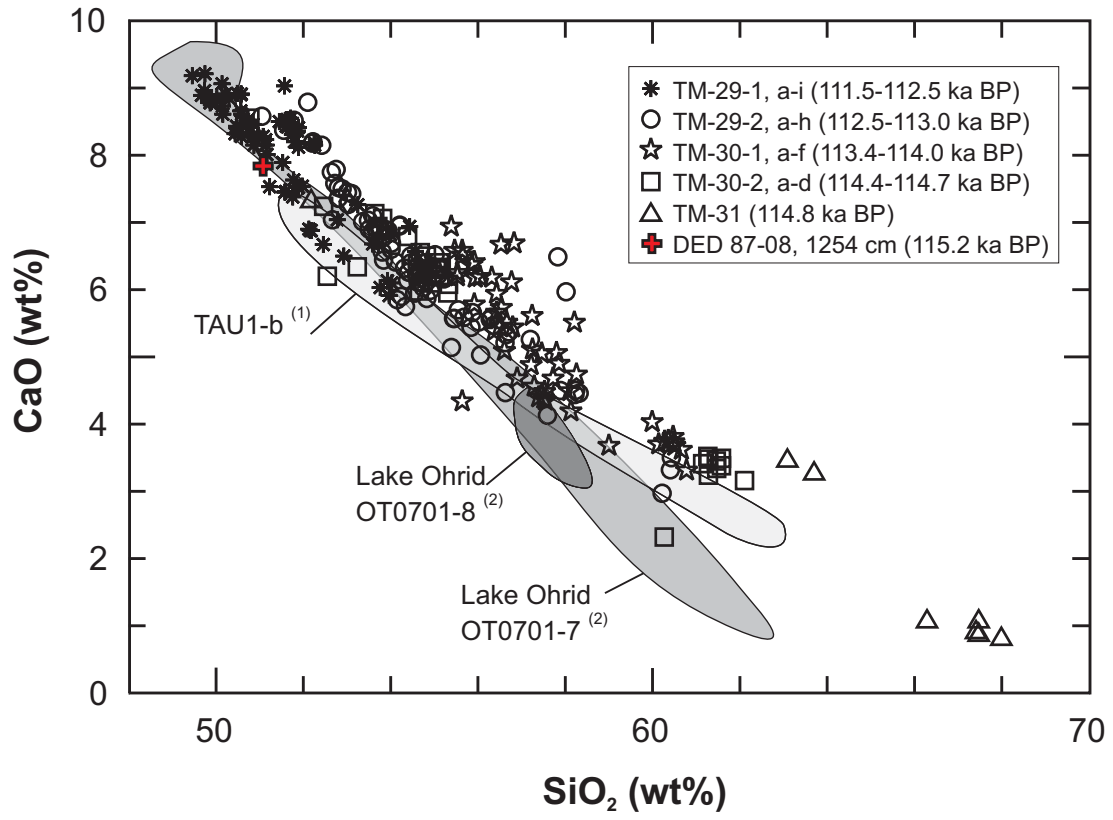


Figure 4c

Figure 4d

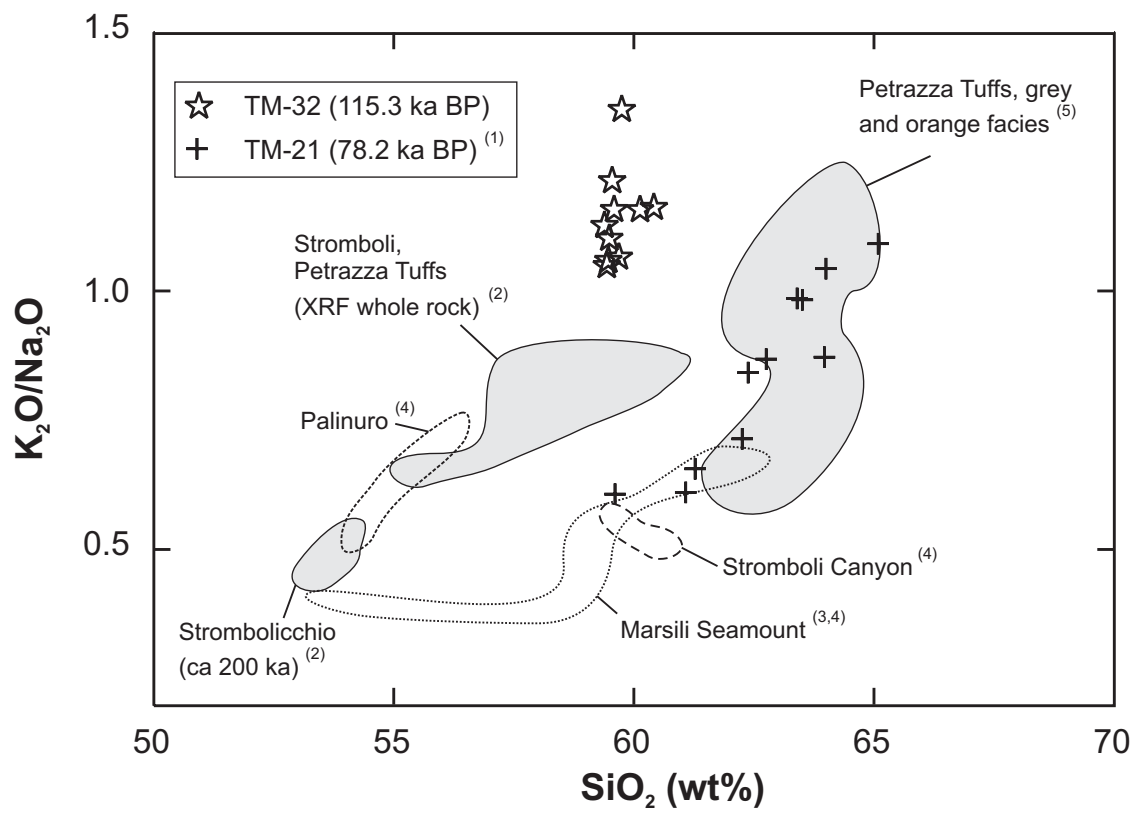


Figure 4d

Figure 4e

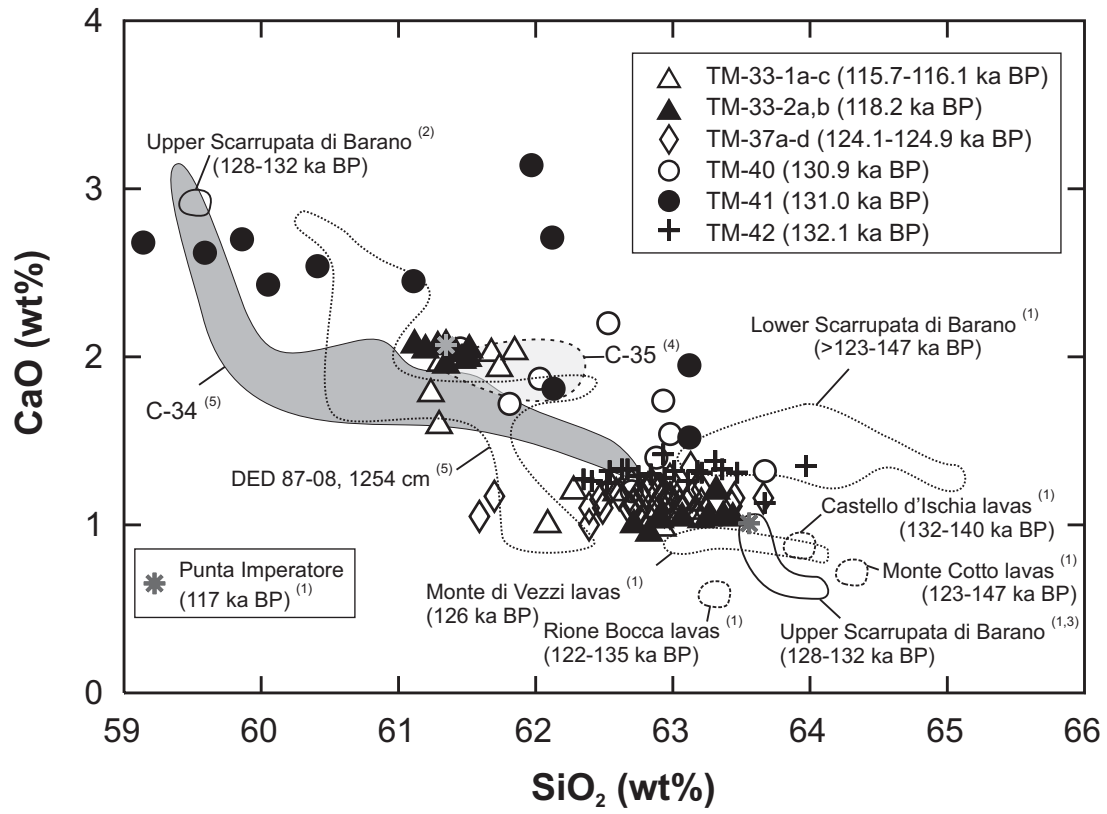


Figure 4e

Figure 4f

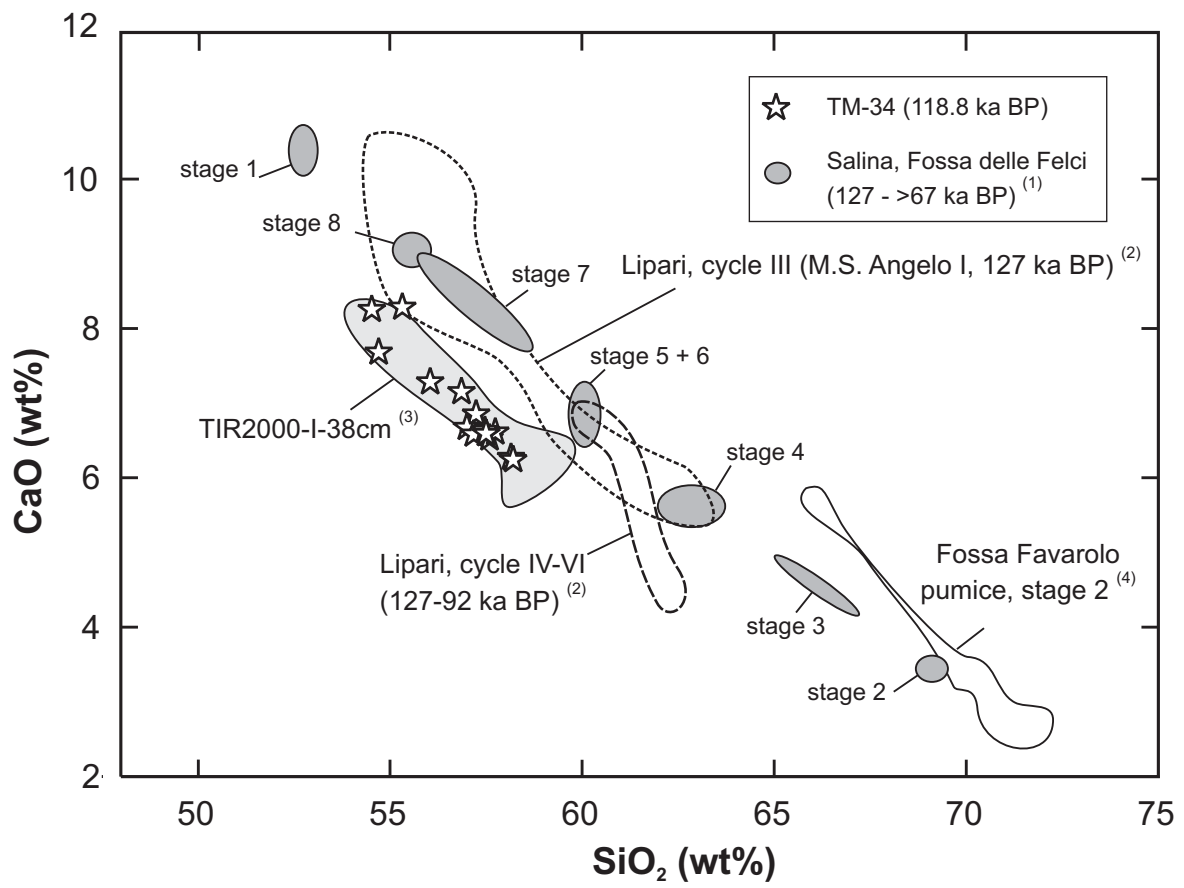


Figure 4f

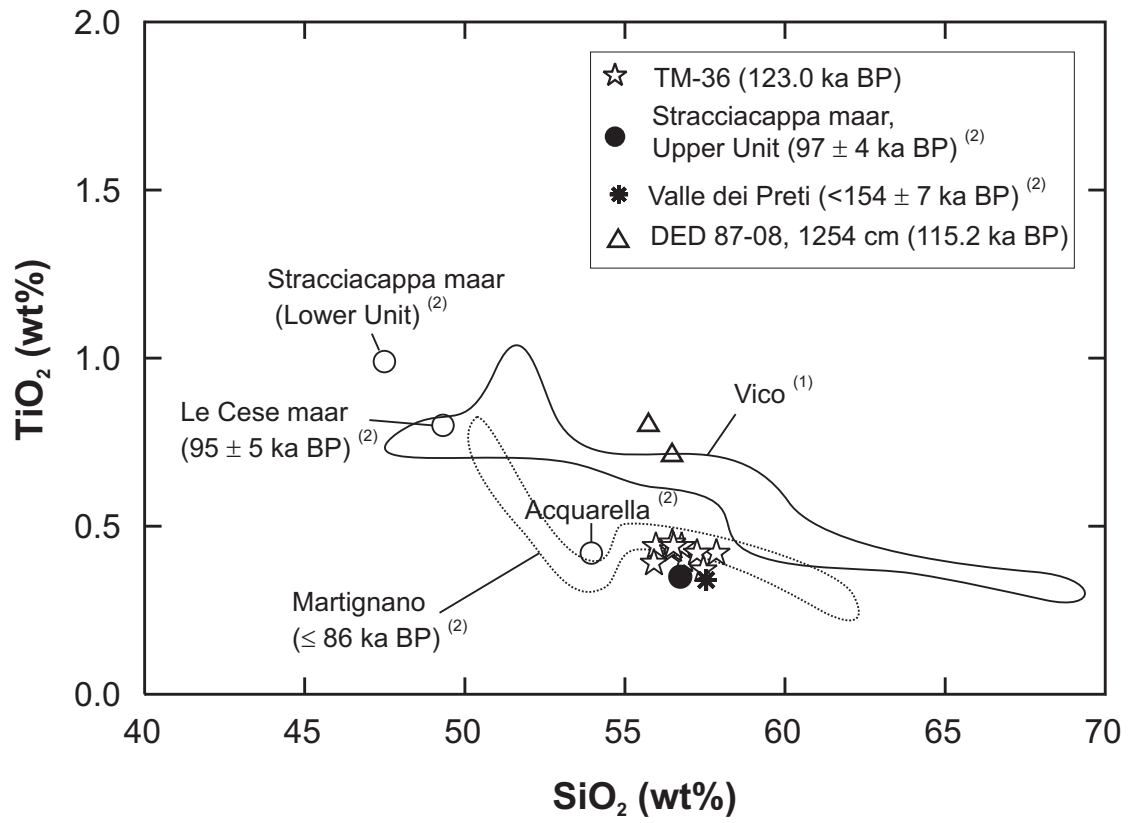


Figure 4g

Figure 5

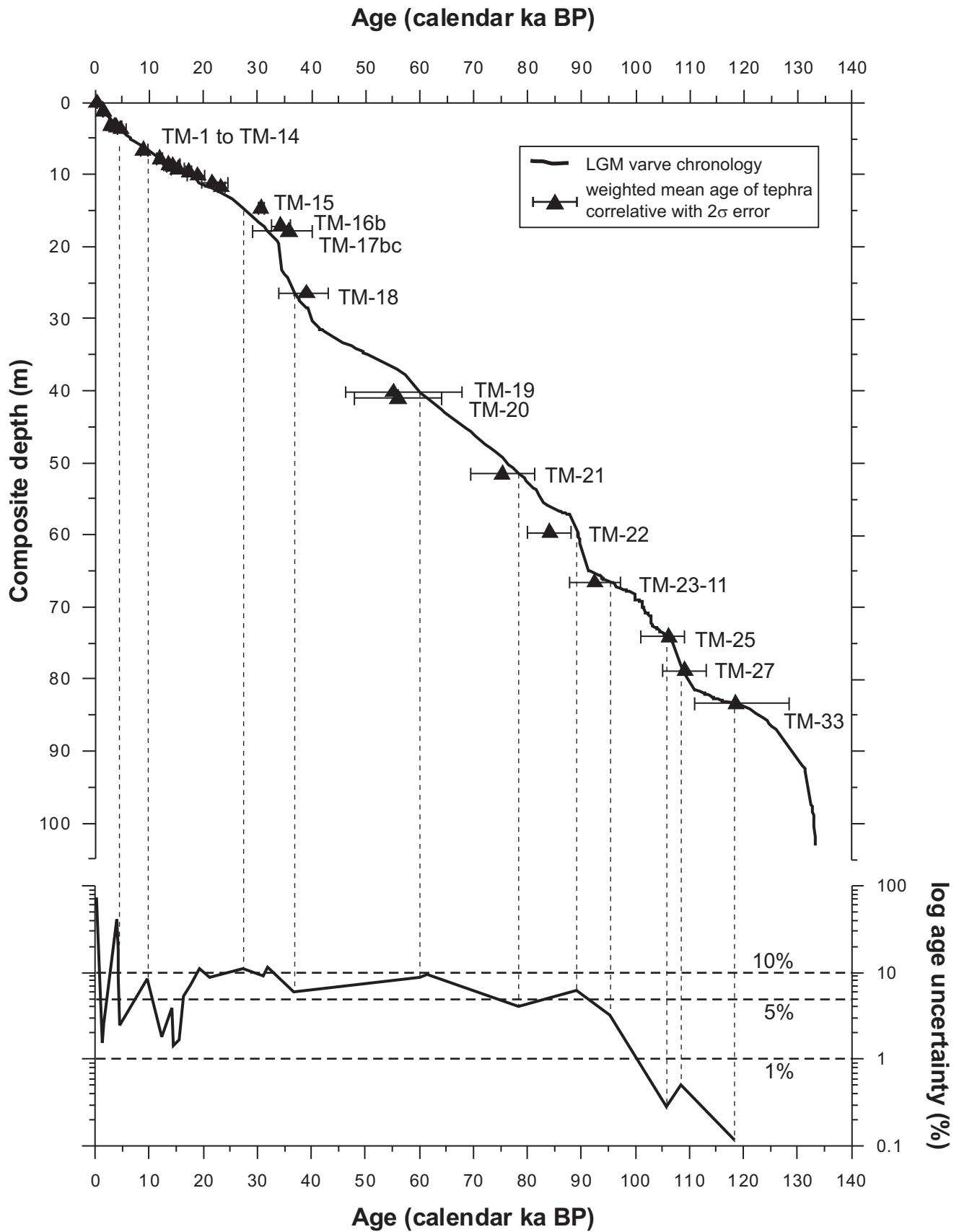


Figure 5

Supplementary Table A

[Click here to download Supplementary Data: Supplementary table A.xlsx](#)

Supplementary Table B

[Click here to download Supplementary Data: Supplementary table B.xlsx](#)

Supplementary Table C

[Click here to download Supplementary Data: Supplementary table C.xlsx](#)